A DENSITY-DEPENDENT MECHANISM FOR ANTIBIOTIC TOLERANCE IN ROD BACTERIA

By

ADDISON ELAINE GRINNELL

Bachelor of Science in Biological Science

Oklahoma State University

Stillwater, OK

2018

Submitted to the Faculty of the
Graduate College of the
Oklahoma State University
in partial fulfillment of
the requirements for
the Degree of
MASTER OF SCIENCE
July, 2021

A DENSITY-DEPENDENT MECHANISM

FOR ANTIBIOTIC TOLERANCE

IN ROD BACTERIA

Thesis Approved:

Dr. Randy Morgenstein

Thesis Advisor

Dr. Tyrell Conway

Dr. Marianna Patrouchan

Dr. Matthew Cabeen

ACKNOWLEDGEMENTS

It has been three and a half years since I've started this program. In that time I've learned so much and have had so many people to thank for getting me to this point. I'll start by thanking my parents who have been there every step of the way and make sure I know they are proud of me. Ross you dealt with the brunt of everything and your jokes, your proofreading, your willingness to do dishes, and your listening ear have gotten me through this. My advisor Randy read through an absurd amount of drafts for every section of this thesis and always had feedback I needed to hear. I hope to be half as good at writing as you are someday. Dr. Elizabeth Ohneck thank you for the many readings and revisions, your expertise and baking has been invaluable. Suman, Ryan, and Brody thank you for all the timepoints you took for me so I could get lunch and for talking to me about whatever random subject came into my head. I'd also like to thank all my friends. There's too many of you to name here but whether you listened to me talk about my work, took my mind off my stress, gave me advice, or all of the above I appreciate you all. To my committee, you always asked the most incisive questions, gave me support and advice constantly, and encouraged me to keep going. There is a myth of the scientist who learned everything themselves, did all the experiments themselves, and figured everything out on their own. I'm proof that is a myth, there are far too many people who helped me through this process for me to even begin to thank. I hope I made you all proud!

Name: ADDISON GRINNELL

Date of Degree: JULY, 2021

Title of Study: A DENSITY-DEPENDENT MECHANISM FOR ANTIBIOTIC TOLERANCE IN ROD BACTERIA

Major Field: MICROBIOLOGY, CELL AND MOLECULAR BIOLOGY

Abstract: The peptidoglycan (PG) cell wall provides shape and structure to most bacteria. There are two systems to build PG in rod shaped organisms: the elongasome and divisome, which are made up of many proteins including the essential MreB and PBP2, or FtsZ and PBP3, respectively. The elongasome is responsible for PG insertion during cell elongation, while the divisome is responsible for septal PG insertion during division. We found that the main elongasome proteins, MreB and PBP2, can be inhibited without affecting growth rate in a quorum sensing-independent density-dependent manner. Before cells reach a particular cell density, inhibition of the elongasome results in different physiological responses, including intracellular vesicle formation and an increase in cell size. This inhibition of MreB or PBP2 can be compensated for by the presence of the class A penicillin binding protein, PBP1B. Furthermore, we found this density-dependent growth resistance to be specific for elongasome inhibition and was consistent across multiple Gram-negative rods, providing new areas of research into antibiotic treatment.

TABLE OF CONTENTS

LIST OF TABLES

Table Page

LIST OF FIGURES

Figure Page

CHAPTER I

INTRODUCTION

The world of bacteria is filled with many shapes and sizes. Why do bacteria even need to have a shape? What benefit does having a shape provide? Form feeds function and function feeds form. The shape bacteria take is broadly uniform within a species and provides different ways of interacting with the environment. Rod bacteria have different advantages than a sphere, a filament has its own set of advantages when compared to either. These advantages allow bacteria to compete for niches and further evolve their fitness for those niches.

Bacteria have a variety of methods to control their shape but the primary one is the cell wall. It is a mesh–like structure that serves a utilitarian role by providing some protection from lysis as a result of environmental stress but also shapes the cell. Cell walls of various chemical compositions serve similar roles across kingdoms of life. For most bacteria the cell wall is necessary for life and growth. It also has a unique chemical composition and method of construction that makes for an important role in treating a bacterial infection.

Pathogenic bacteria are those that can infect and cause disease in other organisms. To treat a bacterial infection antibiotics are necessary. Antibiotics are chemicals that can either stop bacteria from growing or outright kill them. Antibiotics are selected for infections based on the causative bacteria and specificity to bacteria to prevent harm to the host. The cell wall of bacteria is unique to bacteria and essential to life and is a common target for antibiotics. There are several classes of antibiotics target the cell wall in some way at different stages. The usage of antibiotics against infections and commercial agriculture have led to a dramatic increase in antibiotic resistant bacteria.

The mechanisms bacteria can use to evolve antibiotic resistance are many and varied. Many of these mechanisms are worth study in and of themselves because if these mechanisms can also be combatted than so can antibiotic resistance. There are also likely to be uncharacterized methods that can be used by bacteria to develop antibiotic resistance. Bacteria may have the ability to develop resistance to cell wall targeting antibiotics based on how they create and maintain their shapes.

CHAPTER II

REVIEW OF LITERATURE

The Cause and Impact of Cell Shape

The world is filled with innumerable species of bacteria that display a huge diversity of cell shapes and sizes. The diversity of size, shape, and arrangement indicates there are evolutionary niches that can be filled with a selective advantage due to these traits. The most common bacterial shapes are spheres and rods, but can include curves, spirals, branched, filamentous, and cells whose shape eludes simple description (Young 2006). Each of these shapes comes with their own ways of interacting and arranging with other cells, such as chaining or pairing. As with macroorganisms, bacterial form feeds function and function feeds form. Cell shape is tightly controlled within a species, suggesting an important role for cell shape in physiology and thus a mechanism of providing selective advantage. Each shape of bacteria comes with its own system of proteins (or even a single protein) needed to maintain cell shape and in many cases these systems are essential to life (Bean, Flickinger et al. 2009, Esue, Rupprecht et al. 2010).

Cell shape is clearly impactful enough that physiology is warped when proper cell shape is disrupted. The spiral shape of *Helicobacter pylori* is controlled by Csd5

(Krzyżek and Gościniak 2018). When Csd5 is deleted *H. pylori* becomes a straight rod. *H. pylori* infects the mucus lining in the gut and its spiral shape has been shown to be important for colonization as it helps the cells swim through the mucus (Krzyżek and Gościniak 2018). *Caulobacter crescentus* is a curved shaped bacterium whose curvature is a direct result of the protein crescentin (Ausmees, Kuhn et al. 2003). This curved shape allows for greater attachment during conditions of flow and allows WT cells to outcompete straight rods in surface colonization (Ausmees, Kuhn et al. 2003, Persat, Stone et al. 2014).

Bacterial cell shape is primarily determined by the peptidoglycan (PG) cell wall; a complex structure composed of chains of sugars crosslinked via oligopeptides. When cells have the cell wall removed to create L-forms they lose their ability to maintain their wild-type (WT) shape and conversely, when the cell wall is purified from the rest of the cell the purified material maintains the cell shape (de Pedro, Quintela et al. 1997, Joseleau-Petit, Liébart et al. 2007, Cabeen, Charbon et al. 2009). The cell wall does this by forming a flexible but firm net around the inner membrane that keeps the overall shape of the cell to match that of the cell wall. To use an analogy when sewing a stuffed animal, the fabric has its own shape determined by the elasticity of the fabric, its orientation, and where the seams sewn. The stuffing itself is an amorphous blob but the fabric once sewn together will maintain that general shape even without stuffing. The actual architecture of the cell wall varies across species but more importantly across gram structure. Gram-negative peptidoglycan is thinner and uses an oligopeptide crosslink, while Gram-positive bacteria have a much thicker peptidoglycan layer and often use pentaglycine crosslinks in addition to oligopeptide crosslinks.

Biochemistry and Synthesis of the Cell Wall

The glycan portion of peptidoglycan is made up of alternating dimeric subunits of the sugars N-acetylmuramic acid (NAM) and N-acetylglucosamine (NAG), which are mostly found in the cell wall, but NAG can be used in the making of LPS (Heijenoort 2001, Vollmer, Blanot et al. 2008). NAG and NAM must be synthesized in the cytoplasm before being assembled into the cell wall outside of the cell. NAG is formed from fructose-6-phosphate and is then modified with the addition of phosphoenolpyruvate to form NAM. A pentapeptide "stem" attached to NAM is which will eventually allow for crosslinking glycan strands in the cell wall. Both NAG and NAM-pentapetide need to be imported to the periplasm and catalyzed into an alternating chain via a transglycosylase (Chattaway 1982, Heijenoort 2001, Vollmer, Blanot et al. 2008). NAM-pentapeptide is bound to undecaprenyl phosphate forming lipid I. NAG is then attached to the NAM, forming lipid II. Lipid II is then flipped from the cytoplasmic side of the inner membrane (IM) to the periplasmic side of the IM. The NAM-NAG subunit can now be incorporated into the growing PG (Liu and Breukink 2016).

Once in the periplasm parallel, intersecting and vertical layers of glycan chains must be linked to form a stable mesh like structure. The glycan strands are crosslinked by their pentapeptide chains by a transpeptidase enzyme from NAM to NAM to form a tetrapeptide and pentapeptide linked at the third and fourth amino acids respectively. The tetrapeptides used in crosslinking are some of the only places that D-amino acids, D-alanine and D-Glutamate, are found (Cava, de Pedro et al. 2011). Further structure and stiffness arise from the linkage of the outer membrane to the cell wall by Braun's lipoprotein in Gram-negative bacteria. This relationship between the IM and the cell wall

comes most into play during changes to the osmolarity of the environment. The few bacteria without cell walls are extremely sensitive to changes in the osmolarity of their environments and often lyse in hypotonic solutions and shrivel up and die in hypertonic solutions. Modifications to the cell wall are also often necessary in halophile bacteria to prevent plasmolysis.

Crosslinking multiple glycan chains into a single structure provides significant increases in strength and flexibility of the cell wall (Driehuis, de Jonge et al. 1992, Huang, Mukhopadhyay et al. 2008, Rani and Patri 2019). Crosslinking frequency and patterning are related to the strength and elasticity of the cell wall when responding to the physical forces cells are subjected to, such as the tearing forces found in turgor pressure (Huang, Mukhopadhyay et al. 2008, Brill, Hoffmann et al. 2011, Furchtgott, Wingreen et al. 2011, Rani and Patri 2019). Crosslinking frequency is also altered based on physiology. *Escherichia coli* has been known to increase cross-linking in stationary phase (Pisabarro, de Pedro et al. 1985). While tetra peptides are the most common form of crosslink, there is some variation in the number of peptides in the crosslink as well as the particular amino acids that the crosslink occurs on (Quintela, Caparrós et al. 1995, Willey, Sandman et al. 2020). The amino acid composition and pattern of crosslinking often varies by species (Quintela, Caparrós et al. 1995, Boniface, Parquet et al. 2009, Bui Nhat, Gray et al. 2009). This combination of glycan chain length, organization, and crosslinking gives shape, flexibility, and strength to the cell.

The enzymatic heavy lifting of forming glycan chains (transglycosylation) and crosslinking (transpeptidation) is performed by two groups of proteins: penicillin binding proteins (PBPs) and shape, elongation, division, and sporulation (SEDS) proteins. PBPs

fall into two sub-categories; B-class, either a transpeptidase or transglycosylase but not both, or A-class, both a transpeptidase and a transglycosylase. SEDS proteins are typically monofunctional transglycosylases. While the canonical view of peptidoglycan is of an organized grid like structure of crosslinked glycan strands, the recent high-resolution images of the cell wall show that glycan chain organization is not that ordered (Turner, Mesnage et al. 2018). Glycan chain length and organization appear to be correlated with cell shape but not cell wall thickness. Shorter, less organized glycan chains are associated with cocci bacteria and longer more organized glycan chains are found in rod cells (Hayhurst, Kailas et al. 2008, Turner, Hurd et al. 2013, Turner, Vollmer et al. 2014, Turner, Mesnage et al. 2018). However, these experiments have only been done in three species so there is a possibility that this link between glycan chain length/organization and cell shape does not apply more broadly; additionally, there is no knowledge about how curved cells, spirilla, and other shapes arrange glycan chains (Turner, Vollmer et al. 2014).

A Tale of Two Systems: How to Make a Rod Cell

There are two main groups of proteins used by most rod shape bacteria to synthesize PG: the elongasome, which controls lateral cell wall growth, and the divisome, which controls septa formation during fission (van der Ploeg, Verheul et al. 2013, Cho, Uehara et al. 2014). These two systems are broadly homologous to each other. In *E. coli* and many other Gram-negative rods both the divisome and elongasome have an essential modulator (FtsZ or MreB), essential SEDS transglycosylase (FtsW or RodA) with a PBP transpeptidase partner (PBP3 or PBP2), and an A-class PBP (PBP1B or PBP1A) (Adams and Errington 2009, Varma and Young 2009, Shaevitz and Gitai 2010, Cho, Wivagg et

al. 2016). PBP1A and 1B are both non-essential but the double deletion is lethal, suggesting they must be able to compensate for each other. While they have some overlapping function, ΔPBP1B mutants display a slower growth rate and are more susceptible to cell wall targeting antibiotics than ΔPBP1A cells (García del Portillo and de Pedro 1990). These two systems are likely to have some interaction as glycan chain organization is pervasive throughout the cylinder of the cell and the septa (Turner, Mesnage et al. 2018).

The modulator determines the sites of cell wall synthesis and recruits the other proteins in the elongasome or divisome (Adams and Errington 2009). The expression of the modulators is controlled so that both MreB and FtsZ are maximally expressed in log phase and least expressed in stationary phase (Addinall and Holland 2002, Santos, Lobo et al. 2002, Freire, Neves Moreira et al. 2009). MreB is an actin homolog that forms antiparallel membrane associated polymers in order to recruit the other components of the elongasome (Shaevitz and Gitai 2010, van den Ent, Izoré et al. 2014). MreB forms short polymers along the cytoplasmic side of the IM that through its own physical properties and interactions with RodZ, another elongasome component, tend to form in areas of neutral or negative curvature (Salje, van den Ent et al. 2011, Morgenstein, Bratton et al. 2015, Bratton, Shaevitz et al. 2018, Colavin, Shi et al. 2018, Hussain, Wivagg et al. 2018). These sites of polymerization allow for cell wall elongation in the cylindrical portion of the cell. These polymers are dynamic and rotate perpendicularly around the cylinder (van Teeffelen, Wang et al. 2011, Morgenstein, Bratton et al. 2015, Kurita, Shin et al. 2019, Kurita, Kato et al. 2020). These rotational dynamics are only shared by RodZ and RodA, while PBP2 has some conflicting reports in regards to rotation (Vijayan,

Mallick et al. 2014, Morgenstein, Bratton et al. 2015). PBP1A does not share rotation with MreB suggesting it does not require recruitment by MreB for functionality (van Teeffelen, Wang et al. 2011, Lee, Tropini et al. 2014, Morgenstein, Bratton et al. 2015).

Depletion or depolymerization of MreB results in round swollen cells prone to lysis (Bendezú and de Boer 2008, Awuni and Mu 2019). MreB is conditionally essential and can only be deleted under conditions of slow growth/limited nutrient availability (Kruse, Bork-Jensen et al. 2005, Bendezú and de Boer 2008), or when *ftsZAQ* is upregulated (Kruse, Bork-Jensen et al. 2005, Bendezú and de Boer 2008, Cho, Uehara et al. 2014). While it is not clear the exact mechanism for cell lysis after MreB disruption, changes in the surface area to volume ratio combined with loss of cell wall integrity when MreB is disrupted likely explains most of the mechanism for lysis. It is possible that MreB's interaction with the IM and its organization contributes in some way to lysis (Bendezú and de Boer 2008, Salje, van den Ent et al. 2011, Turner, Mesnage et al. 2018). MreB directly binds with the membrane and has been shown to excluded from certain regions of the IM by anionic phospholipids (Lin and Weibel 2016, Shiomi 2017). Similar to actin, MreB has also been linked in organizing and/or associating with integral membrane proteins (Espeli, Nurse et al. 2003, Strahl, Bürmann et al. 2014, Oswald, Varadarajan et al. 2016); however, this in and of itself is not evidence that MreB depolymerization/depletion causes lysis via this loss of membrane interactions. The reasons behind MreB depletion or depolymerization and lysis are relatively unexplored.

Physiology and Cell Shape

An easy to understand and well-studied example of the impact cell shape has on physiology is that of motility (Ferrero and Lee 1988, Cooper and Denny 1997, Maki, Gestwicki et al. 2000, Motaleb, Corum et al. 2000, Kudo, Imai et al. 2005, Young 2006). There are a limited number of cell shapes that allow for different types of motility and efficiency of chemotaxis. For simplicity I will focus on swimming motility (Cooper and Denny 1997, Mitchell 2002). When swimming the viscosity of the environment plays a key role in selection for cell shape. Curved cells result in cells and can move though thicker fluids more efficiently; spirilla also share this trait in viscous environments (Ferrero and Lee 1988, Kudo, Imai et al. 2005, Magariyama, Ichiba et al. 2005, Robertson, Rourke et al. 2005, Bartlett, Bratton et al. 2017). More generally, cocci cells are still capable of swimming but it is very uncommon and bacilli hold an advantage when chemotaxis is involved (Levinson 2018).

Physical forces provide bacilli with a competitive advantage in terms of speed and energy cost involved in swimming possibly due to their hydrodynamic shape, the lesser effects of Brownian motion on rod shape, and their ability to run-and-tumble or reverse to follow a chemical gradient (Cooper and Denny 1997, Dusenbery 1998). The ubiquity of the rod shape and its jack of all trades nature in motility and chemotaxis has its own selective pressure, particularly in length. As rod length increases cells are no longer able to tumble but perform stops and must rely on Brownian motion in order to change direction. The lack of tumbling in filamentous cells puts a pressure on rods that chemotax to be a goldilocks “just-right” size that can respond to chemotactic signals but still tumble to follow a gradient in an efficient way (Maki, Gestwicki et al. 2000). Many rod-shaped

organisms have the majority of their chemotaxis sensory arrays located at the cell poles. As these cells filament, the distance from the pole to flagella increases past the diffusion constant of the chemotaxis response protein (CheY). In filamentous *E. coli*, arrays are found both at the poles and along the lateral wall. This is thought to help position CheY closer to its targets (Silversmith and Bourret 1999). Further constraints on rod size can arise from cell diameter and the energy cost from swimming along gradients, with an inverse relationship between the length of the gradient and diameter of the cell (Mitchell 2002, Takeuchi, DiLuzio et al. 2005). Cell shape effects many aspects of motility and chemotaxis; the energetics, the modes available, and the ability to traverse different environments. This is only one aspect of physiology cell shape has a direct effect on.

Just as cell shape can affect broader aspects of physiology, physiology also affect cell shape. When *E. coli* cells are grown in minimal medium they are unable to grow to the same size as when grown in rich medium (Schaechter, MaalØe et al. 1958, Nanninga 1988). It has been suggested this is a result of growth rate and not necessarily a certain metabolic profile; however, nutrient composition of media directly impacts metabolism to the point where disconnecting the two is very difficult (Nanninga 1988, Lopatkin, Stokes et al. 2019). Upregulation of gluconeogenesis allows cells to survive without properly functioning cell division or elongation in rod cells (Barton, Grinnell et al. 2021). In addition, when glucose is added to media cells become more tolerant to cell wall elongation targeting drugs (Barton, Grinnell et al. 2021). The authors suggest that increased gluconeogenesis in the cell or glucose in the medium leads to the increased synthesis of cell wall precursors which allows alternative pathways to compensate for the inhibition of MreB or PBP2. Work into how β-lactam antibiotics function shows that they

induce a lethal cycle of both halting cell wall synthesis and inducing breakdown of the current cell wall, thereby exhausting the supply of cell wall precursors (Cho, Uehara et al. 2014). Providing glucose or upregulating gluconeogenesis allows for the increased synthesis of cell wall precursors, replenishing those lost by β-lactam treatment allowing other PBPs to increase or continue their activity could provide an avenue to survive these antibiotics.

Bacterial cell shape is much more complex than what has been discussed here. There is a wealth of unique shapes, arrangements, and growth strategies each with their own particular synthesis systems and ecological niche to fill. Rod cells are one of the most common cell shapes and provide a wide variety of advantages such as swimming, chemotaxis, and cell-cell interactions. Many disease-causing agents are Gram-negative rods and therefore understanding these bacteria is crucial to combat these infections (Neu 1985, Breijyeh, Jubeh et al. 2020). The wall is an attractive antibiotic target due to its essentiality and specificity to bacteria, and unique components such as D-amino acids. (Zapun, Contreras-Martel et al. 2008, Worthington and Melander 2013). The essentiality of the cell wall also means that resistance to antibiotics targeting the cell wall is very common and develops frequently and an exploration into how to overcome resistance and how it develops is vital.

A Waiting Game: Methods of Developing Resistance

Antibiotics in a medical setting are necessary for treatment of bacterial infections. However, since the introduction of antibiotics as a common medical treatment antibiotic resistance among bacteria has skyrocketed in frequency (Davies and Davies 2010,

Breijyeh, Jubeh et al. 2020). Resistance to antibiotics is defined by the ability to avoid the deleterious effects of an antibiotic as a result of some change on the genetic level (Depardieu, Podglajen et al. 2007, Davies and Davies 2010, Blair, Webber et al. 2015). The main mechanisms of resistance include modification in a target protein to prevent antibiotic binding, increasing the presence of efflux pumps to remove antibiotics from the cytoplasm, and the synthesis of enzymes to break down antibiotics (Li and Nikaido 2004, Li and Nikaido 2009, Davies and Davies 2010, Worthington and Melander 2013). The pressure to develop antibiotic resistance existed long before human use of antibiotics to treat infections as a result of organisms using antibacterial compounds for a competitive advantage in nature (Aminov and Mackie 2007). For example, the first commercially available antibiotic, penicillin, was discovered from *Penicillium rubens*, a mold. If a resistant mutant/strain of a bacteria is not within the initial population, there are still mechanisms cells can use to avoid killing long enough for cells to develop true resistance (Aminov and Mackie 2007, Davies and Davies 2010, Rajput, Thakur et al. 2018, Levin-Reisman, Brauner et al. 2019).

One survival strategy bacteria have developed for growing on surfaces is the biofilm (Donlan 2002). Biofilms are three dimensional communities of bacteria held together by an extracellular matrix that can occur at the interface of two surfaces when bacteria come into contact with each other (Donlan 2002). This matrix is rather sticky and causes other bacteria to stick to the matrix and begin changing their behavior (Pumbwe, Skilbeck et al. 2008, Rajput, Thakur et al. 2018, Trampari, Holden et al. 2021). Biofilm bacteria also change their physiology and display different phenotypes when compared to planktonic cells such as increases in the expression of efflux pumps (Kvist,

Hancock et al. 2008). Overall biofilm bacteria decrease the killing potential of an antibiotic by physically limiting diffusion of the antibiotic and increasing efflux pump production (DeLisa and Bentley 2002, Li and Nikaido 2009, Rajput, Thakur et al. 2018). This limits the detrimental effects of the antibiotic allowing cells time to grow and evolve resistance over the course of treatment (DeLisa and Bentley 2002, Pumbwe, Skilbeck et al. 2008, Li and Nikaido 2009, Rajput, Thakur et al. 2018, Trampari, Holden et al. 2021).

A common assay for antibiotic resistance or effectiveness is a minimum inhibitory concentration (MIC) assay. It used to determine the lowest concentrations of antibiotic that inhibits cell growth, the MIC. A resistant strain will have a higher MIC of the antibiotic than a susceptible strain (Andrews 2001, McKinnon and Davis 2004). For antibiotics to be effective the target has to be actively growing or dividing (Tuomanen, Cozens et al. 1986, Michiels, Van den Bergh et al. 2016). Therefore, one way the cell can temporarily avoid antibiotic killing is to slow its growth rate or becoming metabolically inert (Handwerger and Tomasz 1985, Windels, Michiels et al. 2019). These methods both have their own nomenclature to make them distinct from resistance; the former is known as antibiotic tolerance and the latter is persistence or persister cells. Tolerance works by slowing down growth rate to also slow down death rate (McDermott 1958, Brauner, Fridman et al. 2016, Levin-Reisman, Brauner et al. 2019). Resistance is distinct from tolerance as resistance arises from some mechanism that increases the concentration of the antibiotic needed to cause a negative effect while tolerance does not change the MIC at all. Tolerance can be innate in a species, be inherited, or caused environmentally. Since MIC assays are an endpoint assay that only assesses the effect of a dose of antibiotic after a significant amount of time, tolerance is harder to detect as it is transient, and tolerant

cells will display the same MIC as a susceptible strain. To detect tolerance, the population is measured consistently over time during antibiotic treatment with tolerant strains displaying a slower but consistent killing when compared to the rapid killing of susceptible cells (Handwerger and Tomasz 1985). In patients, a tolerant strain can still be killed if the patient completes the full length of an antibiotic course but if the patient stops taking antibiotic early these tolerant stains can survive and produce an antibiotic resistant strain (Levin-Reisman, Brauner et al. 2019, Windels, Michiels et al. 2019).

While tolerance can be displayed consistently across a population and result in mutation, persistence is a stochastic phenotype in a population of metabolically inactive non-dividing cells (Bigger 1944, Balaban, Merrin et al. 2004). The percentage of persister cells in a population is relatively consistent within a species and normally very low (Balaban, Merrin et al. 2004, Gefen and Balaban 2009). Persistent cells can "wake up" and become active after the surrounding population of cells is killed off and the antibiotic removed, although the exact mechanism for persister cell waking is debated (Gefen and Balaban 2009, Amato, Fazen et al. 2014, Kim, Yamasaki et al. 2018). Similar to tolerance, the MIC of cells with a persister phenotype is the same as if there were no persister cells since they make such a small proportion of the population (Brauner, Fridman et al. 2016, Levin-Reisman, Brauner et al. 2019). A time killing assay is needed to determine if persistence is occurring (Brauner, Fridman et al. 2016, Levin-Reisman, Brauner et al. 2019). In a time killing assay when an antibiotic is added sensitive cells begin to die; however, at a certain point persistent cells fail to be killed resulting in asymptotic decline of colony forming units. Once the antibiotic is removed these persister cells will awaken and being to grow, although they are still sensitive to the antibiotic if

treatment is readministered. In contrast, tolerant strains display a linear decline in population that is slower than a sensitive strain (Balaban, Merrin et al. 2004, Gefen and Balaban 2009, Harms, Maisonneuve et al. 2016). Persister cells are one of many factors that can lead to chronic infections and antibiotic resistance (Bigger 1944).

The time to accrue mutants in the population is one of the most important factors when discussing mechanisms to develop antibiotic resistance (Tuomanen, Cozens et al. 1986, Aminov and Mackie 2007, Depardieu, Podglajen et al. 2007, Blair, Webber et al. 2015). Tolerance, persistence, and biofilms are all mechanisms that cells can use to temporarily avoid the deleterious effects of antibiotics. These three methods are well characterized and studied and are accepted nomenclature but there is the possibility of more mechanisms both innate and heritable to allow for accumulation of mutations that lead to antibiotic resistance. There are multiple areas worth researching including timing. Persistence and tolerance both show that by altering how cells grow antibiotics become less effective and this could be used to indicate when certain systems of the cell are essential. Normally essential cell systems like the elongasome might lose their essentiality depending on the stage of growth or physiology. This can be exploited to understand these systems better for knowledge about how to improve efficacy or overcome resistance of antibiotics.

CHAPTER III

A DENSITY-DEPENDENT REQUIREMENT OF PBP1B FOR CELLS TO GROW AFTER DISRUPTION OF THE MREB-PBP2 ELONGATION COMPLEX REQUIRES A MINIMUM CELL DENSITY

Introduction

Bacterial cell shape is primarily determined by the peptidoglycan (PG) cell wall, which is made up of sugar polymers cross-linked together by small peptides. Synthesis is catalyzed by a series of penicillin binding proteins (PBPs) with transglycosylase and/or transpeptidase activity (Shi, Bratton et al. 2018). The two main classes of PBPs are class A PBPs (aPBP), which are bifunctional enzymes that can perform both transglycosylase and transpeptidase reactions, and class B PBPs (bPBPs), which are monofunctional transpeptidases. In many rod-shaped bacteria, cell wall synthesis is split among two homologous groups of proteins known as the divisome and the elongasome (van der Ploeg, Verheul et al. 2013). The divisome synthesizes and organizes septum synthesis and is coordinated by the tubulin homolog, FtsZ. The elongasome synthesizes and organizes side wall synthesis during growth and elongation and is coordinated by the bacterial actin homolog, MreB (van Teeffelen, Wang et al. 2011, Shi, Bratton et al.

2018). There is evidence that these two complexes interact with each other (Varma and Young 2009, van der Ploeg, Verheul et al. 2013).

The divisome complex is made up of an aPBP, PBP1B, and an essential bPBP, PBP3. PBP3 works in conjugation with FtsW, a SEDS (shape, elongation, division, sporulation) protein family member (Cho, Wivagg et al. 2016, Meeske, Riley et al. 2016, Leclercq, Derouaux et al. 2017). Interference of the divisome results in long filamentous cells as septation is disrupted (Spratt 1977, Boes, Olatunji et al. 2019). The elongasome complex is made up of a homologous system to the divisome with an aPBP, PBP1A, and the essential bPBP, PBP2 (van der Ploeg, Verheul et al. 2013). PBP2 works in conjugation with the transglycosylase, RodA, its SEDS protein family member (van der Ploeg, Verheul et al. 2013). The polymeric form of MreB directs sites of cell wall remodeling and coordinates the activity of the other members of the elongasome (Bean, Flickinger et al. 2009, Vijayan, Mallick et al. 2014, Hussain, Wivagg et al. 2018, Shi, Bratton et al. 2018). Current work suggests that MreB directly interacts with PBP2/RodA but is independent from PBP1A (Den Blaauwen, Aarsman et al. 2003, Lee, Tropini et al. 2014, Morgenstein, Bratton et al. 2015). The disruption of the elongasome results in dysregulated cell wall insertion during growth, resulting in swollen round cells (Bean, Flickinger et al. 2009).

Interestingly, while disruption of MreB and PBP2 both result in similar round shape changes, they do not share similar overall physiology phenotypes (Cho, Uehara et al. 2014, Barton, Grinnell et al. 2021). MreB was discovered in screens for mutants resistant to the PBP2-targeting drug, mecillinam (Wachi, Doi et al. 1987). Antibiotics targeting PBPs, such as mecillinam and other beta-lactams, induce a futile cycle by both

inhibiting new cell wall synthesis and inducing breakdown of the current cell wall, while inhibition of MreB with the drug A22 does not induce breakdown of the cell wall (Uehara, Parzych et al. 2010, Cho, Uehara et al. 2014).

MreB is conditionally essential and deletion can only be achieved by very slow growth or with the accumulation of suppressors, such as the upregulation of *ftsZAQ*. However, during stationary phase the transcriptional repressor BolA can repress *mreB* expression (Aldea, Hernández-Chico et al. 1988, Santos, Lobo et al. 2002). Ectopic expression of *bolA* during exponential phase leads to a round cell phenotype similar to that seen when MreB is depolymerized by A22 (Freire, Neves Moreira et al. 2009). From this, we hypothesized that MreB might be dispensable and therefore less sensitive to A22 during stationary phase when BolA should be most actively repressing its expression.

As expected, addition of A22 to cells after six hours of growth resulted in no change to growth rate; however, we found that A22 can be added as early as 2 hours after inoculation without affecting the growth rate of cells. Here, we show that the effects of A22 on cell growth work in a quorum sensing (QS)-independent, cell density-dependent manner, while loss of cell shape is independent of cell density. Furthermore, this cell density-dependent growth resistance is only seen when the elongasome components MreB and PBP2 are targeted, but not other cell wall synthesis proteins. We show that the ability of cells to continue to grow as round cells requires the activity of the divisome protein PBP1B. Additionally, this cell density-dependent growth resistance (DDGR) appears in other MreB-containing Gram-negative rod species.

Results

Timing of A22 addition is important for growth rate changes

MreB is essential for rod shape in many bacteria. It is thought that MreB organizes the localization of the cell wall synthesis machinery; therefore, MreB should be at maximal expression and activity during exponential phase when cells are growing the fastest. In *E. coli*, the transcription factor BolA is most active during stationary phase (Freire, Neves Moreira et al. 2009). It has been shown that BolA can repress transcription of MreB, contributing to the change in length:width ratio in stationary phase cells (Morgenstein, Bratton et al. 2015, Bratton, Shaevitz et al. 2018). Therefore, we hypothesized that disrupting MreB with the depolymerizing agent A22 when cells are close to stationary phase will have less of an inhibitory effect on cell growth than when cells are disrupted with A22 in exponential phase (Awuni and Mu 2019).

To test our hypothesis, we performed growth curves with wild-type (WT) E. coli with the addition of A22 (10 µg/ml) every hour from T0-6 (Fig. 1A). As we anticipated, the addition of A22 near stationary phase (T5-6) showed little to no change in growth rate. Surprisingly, when A22 was added during log phase, we observed little change in growth rate when compared with the LB only control (T2-4). Only cells still in lag phase (T0-1) showed a marked difference in growth after A22 addition. T3 will be used going forward to test this A22 inoculum time effect unless otherwise stated. Therefore, any differences in growth due to the time of inoculation are most likely independent of BolA as *bolA* is not observed to be expressed until T4 (Aldea, Garrido et al. 1989).

Disruption of MreB by A22 should lead to round cells (Gitai, Dye et al. 2005, Awuni and Mu 2019). We compared the cell shape characteristics of sensitive cells (T1) treated with A22 to resistant cells (T3) treated with A22. Cells were imaged every hour for seven hours with and without A22 added at T1 or T3 (Fig. 1B). To quantify the change in rod shape, we measured the intracellular diameter deviation (IDD); a larger IDD indicates cells are less rod shaped and more round (Bratton, Shaevitz et al. 2018). Interestingly, both T1 and T3 A22 treated cells become equally round in roughly the same amount of time after treatment (Fig. 1C) suggesting there is no difference in the degree and speed of MreB depolymerization in sensitive or resistant cells.

Surprisingly, although both T1 and T3 treated cells become round after A22 addition, the size of the cells is different. The cell area of T1 treated cells more than doubles (4.30 to 9.82 μm^2) within the first two hours of A22 treatment, while T3 treated cells become slightly smaller (5.06 to 4.31 μm^2) during that same length of A22 treatment (Fig. 1D). T1 treated cells do not grow during the time course as the cell area actually decreases (9.88 to 5.89 μm^2); however, T3 treated cells show a slight increase in cell area (3.21 to 4.47 μm^2) during the time course suggesting that these cells are still able to grow.

We also observed that cells treated with A22 at T1 commonly develop intracellular vesicles (Fig. 1B arrows) suggesting they are in the early stages of lysis (Berman-Frank, Bidle et al. 2004). We hypothesize this decrease in cell size seen in T1 treated cells is a result of larger cells lysing, leaving only smaller cells to measure. Unlike T1 treated cells, T3 treated cells rarely develop vesicles (0.4-0.5%). These data suggest there are physiological differences between cells treated with A22 and T1 versus T3.

Growth resistance to A22 is due to cell density

Cells are able to grow at normal rates when A22 is added at T3 but not T0/1. There are many factors that are different between the cells at these time points. First, cells are growing faster at T3 (log phase) than they are at T0 (lag phase). To test if growth rate is responsible for the observed growth differences in A22, we grew cells at 30°C to slow down the growth rate. A22 was added to one culture at T0 and one when the culture reached an equivalent O.D.600 (~0.1) as when the cells were grown to T3 at 37°C (Fig. 2A). Additionally, we slowed down the growth rate by growing cells in M63-lactose minimal media (37°C) to an $O.D._{600}$ of 0.1 (Fig. 2B). In both conditions of slower growth rates, cells were able to grow better when A22 was added at the later time point than at T0 (Fig. 2AB). These results suggest that differences in growth rate are not the likely cause for A22 resistance at T3.

Next, we investigated whether growth phase was responsible for the WT-like growth in A22, as T0 cells are in lag phase and show reduced growth while T3 cells are in exponential phase and are able to grow at a rate as if they were in LB only medium. To mimic the growth conditions of cells at T3, we sub-cultured cells grown to T3 into pre-warmed media with A22 (LB_{A22}) and without (LB) A22 (Fig. 3A). At a 1:100 dilution of T3 cells, A22 causes a significant reduction in growth rate, leading us to conclude that exponential phase alone is not the reason for continued growth after A22 addition. We then determined if different sub-culture dilutions would show similar results. Interestingly, 1:1 and 1:10 dilutions grow the same whether or not A22 is present (Fig. 3A). A major difference between the different dilutions is the number of cells present; therefore, we hypothesized that cell density was responsible for the observed growth

resistance. However, as smaller dilutions allow for less mass doublings before cells reach stationary phase, it is possible the due to the slow action of A22 the number of possible mass doublings results in the differences in growth.

To test this, we repeated the back dilution experiment with cells grown to an $O.D._{600}$ ~0.1. These cells were backdiluted 1:1 into prewarmed media with and without A22 and allowed to grow again to an $O.D._{600}$ ~0.1. This was repeated for a total of five "generations" (Fig. 2C). There is no observed growth defect due to A22 over the course of these "generations" despite allowing cells to have more time in exponential phase and therefore more mass doublings. This further suggests that the slow action of A22 is not responsible for the observed growth differences.

To test the effect of cell density on the ability of the cells to continue to grow in A22, we grew cells in A22 in two ways: 1) using different inoculation ratios from an overnight culture, and 2) using different starting O.D.s to begin the growth curves, both with A22 the entire time. Our previous growth curves began with a 1:1000 dilution of an overnight culture. We decreased this dilution factor by an order of 10 or 100 and saw a decrease in the difference of growth rates between cells grown in A22 medium compared to medium alone as the dilution factor increased, supporting our hypothesis that cell density is important for growth in A22 (Fig. 3B). Cultures starting with specific O.D.s also show a density-dependent growth phenotype, further supporting the role of cell density in A22 growth resistance. To avoid any media affects, an overnight culture was washed in fresh media before cells were inoculated in media with or without A22 at an $O.D._{600}$ of 0.1 (~ the same as T3 cells), 0.05, 0.025, and 0.0125. The higher starting density cells show no growth difference with or without A22 (Fig. 3C, Table 1).

However, inoculation of cells at lower O.D.s results in a change in growth rate when A22 is added. (Fig. 3C). To quantify the growth rate changes at the different starting O.D.s we measured the exponential grow rate of cells from each dilution and compared the growth in media with and without A22 (Table 1). These results show that the difference in growth rates between media with and without A22 is only statistically significant when the cell density is low; at higher starting O.D.s there is no difference in growth between media with and without A22. These data further refute the idea that growth phase is important for the growth-resistance, as all cells are starting in lag phase, independent of starting inoculum density, and support the hypothesis that the ability of *E. coli* to grow as round cells with disrupted MreB is dependent on cell density. In addition, all starting $O.D._{600}$ conditions grew linearly for similar amounts of time and only the lower cell densities showed growth defects, implying there was an equal amount of mass doubling for A22 to have an effect.

As modulating cell density phenocopies the A22 growth pattern that was initially observed for cells treated at different time points (Fig. 1 and Fig. 3C), we tested if increasing cell density results in the same physiological changes to A22 treatment: vesicle formation and cell size. Cells were grown from a starting $O.D._{600}$ of ~0.1 or 0.01 in LB or LB_{A22} and imaged every hour for four hours (Fig. 2E, 3D). Unlike our previous experiment, this set up also accounts for differences in length of A22 exposure as all cultures received A22 at the beginning of the assay. Both treated cells become round at the same rate and to the same degree when treated with A22, supporting the idea that the degree and speed of MreB depolymerization is unchanged (Fig. 3F). Interestingly, 0.1 cells did not become as large as their 0.01 counterparts (Fig. 3E), similar to what was

seen for T1 and T3 cells (Fig. 1D). Although both inoculation densities result in vesicle formation, the low density cells form vesicles earlier and at a higher frequency than the high density cells (Fig. 3D). These data support the hypothesis that cells at different densities have different physiological responses to A22. We will refer to this phenomenon as density-dependent growth resistance (DDGR).

It is possible that cells might serve as a sponge or reservoir for A22 by physically adsorbing the A22 to the membrane or collecting it in their cytoplasm thereby diluting out the drug. To test this idea, we artificially increased the starting O.D. of a culture with intact heat killed cells (inset Fig. 2E). Heat killed cells were added to fresh media at an O.D. of 0.4, a concentration >4X what is needed to observe A22 growth resistance. Cells grown overnight were sub-cultured 1:1000 into this culture with and without A22. The presence of heat killed cells did not protect the sub-cultured cells from the A22, as there is an obvious separation of growth between the LB and LBA22 media (Fig. 2E). This suggests that some component of live cells is responsible for DDGR. In addition, DDGR does not go away even with a 5X increase in the A22 concentration added at T3 (Fig. 4A) supporting the idea that physiological differences exist between cells at different densities.

Changes in the media are not responsible for A22 growth resistance

Our results suggest that cell density is important for A22 growth resistance. Because we washed the overnight cells before use, we did not think QS or media changes were involved. However, to specifically test a role for QS, we grew cells in 10% spent media from overnight cultures with and without the addition of A22 (Wang, Liu et al.

2019). The addition of 10% spent media did not confer resistance to cells grown in A22 (Fig. 5A), suggesting that QS is not involved in A22 growth resistance.

As cells grow, they induce other changes in the medium, such as a decrease in pH, an increase in waste products, and the removal of nutrients (Maseda, Sawada et al. 2004, Pumbwe, Skilbeck et al. 2008, Lobritz, Belenky et al. 2015, Lopatkin, Stokes et al. 2019, Mueller, Egan et al. 2019). To test if any of these changes were occurring and responsible for the increased growth in A22, we grew cells with A22 in 100% partially spent media from cells grown to an O.D.600 ~0.1 (T3). As cells at T3 exhibit DDGR, if the resistance is due to the media conditions at this time point, freshly inoculated cells should also exhibit A22 growth resistance. We found no difference in growth in cells treated with A22 in the 100% partially spent media vs the fresh media (Fig. 5B). These results suggest that, while living cells are required for DDGR, cells are not making a diffusible product nor are they changing the media to induce resistance.

Cell density provides resistance to PBP2 disruption

A22 is not a clinically used antibiotic; therefore, we wanted to determine if DDGR is common among other antibiotics, including those used clinically. We tested E. coli cells grown to T3, to equalize time of drug exposure, and added inhibitory doses of antibiotics targeting cell wall synthesis (A22, mecillinam, cephalexin, cefsulodin, phosphomycin, ampicillin), translation (kanamycin, chloramphenicol, gentamicin, tetracycline), and transcription (rifampicin) (Fig. 6A). The translation- and transcription-targeting antibiotics arrest growth within 30 minutes of the addition of the antibiotic, while the cell wall-targeting antibiotics cause more variations in response. Phosphomycin

and ampicillin both cause active cell lysis within an hour after addition while cells treated with cefsulodin and cephalexin grow for an hour before growth is inhibited; however, mecillinam (mec), which specifically targets PBP2, is the only tested antibiotic that phenocopies the A22 DDGR phenotype. As MreB (target of A22) and PBP2 (target of mec) interact with each other, it is logical that they both show this phenomenon when targeted by their respective antibiotics (Den Blaauwen, Aarsman et al. 2003, Rohs, Buss et al. 2018).

Similar to A22, mec also causes treated cells to become swollen and round (Fig. 7), confirming that mec is still active when added at higher cell densities. To confirm that the concentration of mec used is high enough to kill cells when added at lower O.D.s, we performed a growth curve analysis with mec added at T0 and T3. The concentration of mec used is high enough to almost abolish all growth when added at T0 but shows almost no effect when added at T3 (Fig. 8B).

It has been reported that cephalexin causes a similar density-dependent resistance as we have observed for A22 and mec (Greenwood and Grady 1975, Chung, Yao et al. 2009). Because we did not observe cephalexin to have DDGR we replicated the experiment of Chung et al. which grew cells at different starting dilutions with cephalexin (Chung, Yao et al. 2009). It was reported that cephalexin has no effect when a 1:100 starting dilution is used compared to a 1:1000 dilution. Repeating this experiment, we do not see the same growth in cephalexin at an initial inoculation of 1:100. However, if we use a 1:10 starting dilution we are able to recapitulate their results (Fig. 8A). In this respect, we believe that resistance to cephalexin at a 1:10 inoculation ratio is likely a

result of limited mass doublings as these cells barely grow and is a different phenomenon than DDGR reported here.

To determine if the DDGR seen with mec treatment was due to mec itself or the inhibition of PBP2, we used a temperature sensitive mutant of PBP2 (PBP2ts) (Woldringh 1988). At temperatures >40oC, the PBP2ts mutant grows slowly, and the cells are round, while at the permissive temperature (30^{o}C) the cells grow as rods. To test if the growth defect associated with the loss of PBP2 is density dependent, we started both WT and PBP2ts cultures growing at 30^{o}C and shifted them to 40^{o}C every hour for four hours. If there is a DDGR phenotype, the change in growth rate after the shift to the higher temperature should be greatest when cultures are shifted early, before the proper density is reached. As a control, we grew the WT and PBP2ts cells at both temperatures the entire time (Fig. 8BC). WT cells are able to grow well at both temperatures, while the PBP2ts strain has reduced growth at 40^{o}C. In order to determine how growth was affected by the shift in temperature, we measured the ratio of growth rates of each strain before and after the temperature shift (Fig. 8D). For cultures shifted at T1 and T2, there were not enough data points to calculate a growth rate during the 30^{o}C growth period; therefore, we used the growth rate of the control sample. In support of our density-dependent hypothesis, at all time points, WT cells show an increased growth rate when shifted to 40oC (above 1 Fig. 8D), while the PBP2ts mutant grows worse after the shift for the first two hours (below 1 Fig. 8D). After three hours of growth at the permissive temperature, the change in growth rate caused by the temperature shift was minimal, likely due to the cells being at a high enough density for DDGR (Fig. 8C-D). This result, in conjunction with the mec and A22 experiments, further supports the hypothesis that

the elongasome can be disrupted at higher cell densities without deleterious effects on cell growth.

With two essential components of the elongasome displaying DDGR we sought to test RodA, the essential transglycosylase partner of PBP2, for DDGR (Bendezú and de Boer 2008, Meeske, Riley et al. 2016). While there are no antibiotic compounds we are aware of that can inhibit RodA, there is a temperature sensitive mutant (Matsuzawa, Hayakawa et al. 1973). As such, we performed the same temperature shift experiment with RodAts cells as we had with PBP2ts cells. WT cells displayed the same pattern of growth in shifts as they had previously (Fig. 8E). While RodAts cells grew more poorly overall, they still display better growth at 40ºC after later shifts (Fig. 8G). Interestingly, the T1 shift results in cells stopping growth and lysing before growth continued (Fig. 8F). These results support the model that the specific inhibition of the elongation machinery can be overcome in a density-dependent manner.

PBP1B compensates for disruption of the elongasome

In addition to the MreB-PBP2-based elongasome complex, there are other cell wall synthesis enzymes, including PBP1A and PBP1B. Unlike PBP2 which only has transglycosylase activity, PBP1A and PBP1B have both transglycosylase and transpeptidase activity (Born, Breukink et al. 2006, Barrett, Wang et al. 2007, Egan, Jean et al. 2014). While PBP1A and PBP1B can compensate for each other, they are proposed to have different functions, with PBP1B being in the divisome and PBP1A working independently of MreB during elongation (Vijayan, Mallick et al. 2014, Morgenstein, Bratton et al. 2015). We have recently shown that a mutation in malate dehydrogenase,

mdh, is more tolerant to A22 and mec and that this increased resistance is possibly due to the increased activity of PBP1B (Barton, Grinnell et al. 2021). Therefore, we sought to determine if either PBP1A or PBP1B is needed for continued growth after A22 or mec treatment at higher cell densities.

We tested ΔPBP1A and ΔPBP1B deletions for their ability to continue to grow after spikes of A22 or mec at $O.D._{600}$ ~0.1 compared with the addition of A22 at T0. When spiked with either A22 or mec, ΔPBP1A cells continue growing at the same rate as the LB-only control. However, the ΔPBP1B cells stop growing within an hour and eventually lyse when spiked with A22 or mec (Fig. 9AB), supporting previous reports (Sarkar, Dutta et al. 2012, Thulin and Andersson 2019). These data suggest that PBP1B is needed for DDGR of both A22 and mec treatments.

We noticed that the PBP1B deletion cells are more sensitive to both A22 and mecillinam when added at T0 (Fig. 9AB). To confirm that the lack of DDGR to mec and A22 in the PBP1B mutant is not a result of its increased sensitivity to these drugs, we checked if other A22-sensitive mutants maintain DDGR. To our knowledge, there are no known mutations outside of MreB that increase sensitivity to A22; therefore, we performed an A22 sensitivity screen on the Keio collection in order to find such mutants (Baba, Ara et al. 2006).

From this screen, we have confirmed two mutants with increased sensitivity to A22: *envC* and *yccK* (*tusE*) (Fig. 10A). EnvC is an activator of cell wall hydrolases needed to separate daughter cells after division (Uehara, Parzych et al. 2010). Due to the suspected role of PBP1B in survival after A22 or mec treatment and PBP1B's proposed

role in cell division, we decided to focus on the *tusE* deletion as our control sensitive strain. TusE is a sulfur transferase involved in modification of tRNA and is therefore a good candidate to use as a control for these experiments (Ikeuchi, Shigi et al. 2006). We tested ΔtusE cells for their ability to survive a spike of A22 or mec at an $O.D._{600}$ ~0.1 and found no reduction in growth despite the heightened sensitivity of these when the drugs are added at T0 (Fig. 8B and 9C). This indicates that the inhibition of growth and lysis after the addition of A22 or mec at later timepoints is due to the lack of PBP1B and is not a universal feature of strains more sensitive to A22 or mec.

Previous data has shown that overexpression of cell division proteins suppresses the growth defects of an mreB deletion (Kruse, Bork-Jensen et al. 2005, Bendezú and de Boer 2008). Our current work shows a role for PBP1B in survival of cells treated with A22, further suggesting that the divisome is important during growth and not just division (Fig. 9AB). To further test the importance of the divisome during A22 treatment, we treated cells with combinations of A22 and antibiotics that inhibit a divisome component: cephalexin (FtsI), cefsulodin (PBP1A/B), or a control: kanamycin (30S ribosomal subunit). We used a dose of each antibiotic that is closer to the minimum inhibitory concentration (MIC) and lower than what was used in figure 4 (cephalexin, 5 μg/ml; cefsulodin, 7.5 μg/ml; and kanamycin, 3.12 μg/ml), to more easily determine changes in growth due to A22. Each drug was added when cells reached an $O.D._{600}$ ~0.1 alone or in combination with A22. When cells are treated with this lower concentration of cephalexin there is minimal growth inhibition. However, when A22 is added at the same time cell growth is dramatically reduced. When cefsulodin is used alone, cells stop growing after ~2 hours, but when A22 is added with cefsulodin, cells stop growing within

1 hr and reach a lower O.D. The kanamycin control-treated cells stop growing after the addition of the drug, but when kanamycin is combined with A22, cells do not display an increase in sensitivity compared to the kanamycin only treated cells (Fig. 9D). These data show that inhibiting divisome components, but not other cellular targets, blocks the A22 density-dependent growth resistance phenotype, supporting the idea that the divisome is needed for growth after disruption of MreB and reinforcing a role for PBP1B in DDGR.

A22 spike resistance is common in MreB rod species

MreB is highly conserved in many rod-shaped organisms, including multiple human pathogens making a potential target for antibiotic development. To assess if DDGR is a common phenomenon among MreB containing bacteria we tested two human pathogens, *Shigella flexneri* and *Pseudomonas aeruginosa*. We performed growth curves using both P. aeruginosa PA01 and S. flexneri with A22 added either at T0 or an O.D.600 ~0.1 (Fig. 11). Like *E. coli*, both species continued to grow similar in LB and LB_{A22} only after the addition of A22 at $O.D._{600}$ ~0.1. Both species grew worse when A22 was added at T0, further supporting a role of cell density in resistance to A22. We show that DDGR to the loss of MreB is found across three distinct genera indicating a common novel mechanism for growth during elongasome inhibition.

Conclusions

MreB is necessary for proper cell shape in many rod-shaped bacteria. MreB polymers are critical for proper insertion of PG in rod shaped cells, as they are thought to organize the localization of the cell wall synthesis enzymes (van Teeffelen, Wang et al. 2011, Vijayan, Mallick et al. 2014, Shi, Bratton et al. 2018). We therefore hypothesized that rapidly

growing cells, such as those in exponential phase, would be more sensitive to disruption of MreB than slow growing cells, such as those in stationary phase. In fact, the transcriptional repressor BolA reduces MreB levels during stationary phase (Santos, Lobo et al. 2002, Freire, Neves Moreira et al. 2009). To test this idea, we added the MreB depolymerizing drug A22 during the beginning and end of exponential phase expecting to see less of an effect as cells approached stationary phase. Surprisingly, we found no growth defect when A22 was added in early exponential phase (Fig. 1A). Furthermore, the growth resistance seen in response to A22 treatment is a result of cell density. DDGR to the loss of the elongasome is only possible when PBP1B is present.

A22 growth resistance is dependent on cell density

Cells treated with A22 at the time of inoculation (T0) show a growth defect, but cells treated with A22 2-3 hours after inoculation continue to grow at the same rate as cells in LB only medium (Fig. 1A). Cells treated at T1 become much larger and stay that size compared to those treated at T3 which continue to grow in size after A22 treatment. Additionally, T1 cells develop intracellular vesicles, indicating the beginning of cell lysis (Fig. 1B), while T3 cells do not (Berman-Frank, Bidle et al. 2004). It is unclear why the timing of A22 treatment causes such a drastic change in cell area and vesicles formation, but this suggest differences in the physiological state of the cells and may lead to insights into the cause of survival differences (Fig. 1B, C and Fig. 2 D, E).

We have shown that growth phase is not responsible for DDGR as the dilution of exponential phase cells results in sensitivity and lag phase cells can be resistant when inoculated at different cell densities. (Fig. 2). Together these results suggest a density-

dependent mechanism for growth resistance. Because it is possible that higher amounts of cells lead to dilution of the antibiotics, we added 5X more A22 and 33X more mecillinam (Fig. S2) without losing DDGR, suggesting that the increased number of cells are not diluting out the antibiotic. Finally, temperature sensitive mutants of both PBP2 and RodA show DDGR without the use of drugs (Fig. 4 B-G).

Cell-cell interactions might play a role at higher cell densities but given that all experiments took place under conditions of shaking liquid media, any cell-cell contact is likely to be brief. It is possible that the likelihood of cell-contact increases in a density-dependent manner even in shaking culture; however, other cell-contact-dependent phenomena such as killing via type VI secretion or conjugation occur on solid media but not in liquid (Achtman, Kennedy et al. 1977, Zahrl, Wagner et al. 2006, Aoki, Webb et al. 2009).

It is suggested via BolA's activity that cells in stationary phase and therefore at T0 should have less MreB (Santos, Lobo et al. 2002, Freire, Neves Moreira et al. 2009). It is possible that the lower amount of MreB potentially increases the effectiveness of A22, as there would be more A22 per each MreB polymer per each cell; however, we don't believe this explains DDGR as multiple experiments have shown a density dependency of cells in different growth phases. In testing the role of exponential phase in DDGR we saw that log phase cells (high MreB concentration/cell) and stationary phase cells (low MreB concentration/cell) can be desensitized to A22 (Fig. 2A-C) by simply changing the cell density: indicating DDGR is not related to the ratio of drug to target protein.

Changes in the media are not responsible for density-dependent growth resistance

A non-biological difference cells encounter between T0 and T3 are changes in the media. When cells grow in LB, they exhaust certain nutrients in a stepwise fashion. When one nutrient is exhausted, they alter their metabolism and that shift in metabolism can alter physiology and potentially A22/mec resistance (Falagas, McDermott et al. 1997, Mueller, Egan et al. 2019). Additionally, as bacteria metabolize amino acids, they lower the pH of the media and lower pH has been linked to increasing MICs (Falagas, McDermott et al. 1997). That cells grown in spent media from $O.D._{600}$ ~0.1 cells still display sensitivity to A22 at T0 and DDGR at T3 (Fig. 2C) further supports the idea that changes to the media are not the cause of DDGR. To further our conclusions about pH we have also performed experiments in MOPS (Fig. 2C) and M63 minimal media (Fig. S1) which do not show as dramatic of pH changes as seen in LB. Therefore, we can conclude that nutrient exhaustion and pH changes are not the cause for DDGR.

A common cell density-dependent phenomenon is quorum sensing (QS). QS has been linked to antibiotic resistance via efflux pump activity, and biofilm formation (Pumbwe, Skilbeck et al. 2008, Rajput, Thakur et al. 2018, Wang, Liu et al. 2019). We have shown that QS is not involved in density-dependent growth resistance (DDGR). When 10% overnight spent media was used, we saw no change in growth between A22 and LB only media at T0 (Fig. 3B). Additionally, when treated with A22 at T3 the cells growing in 10% spent media displayed the same growth rate as those in fresh LB. These data suggest that DDGR is not due to QS.

PBP2 inhibition displays density-dependent growth resistance

To determine if DDGR is a common feature of other antibiotics, we tested 10 additional antibiotics with a variety of cellular targets (Fig. 4A). DDGR was only observed in A22 and mec, which targets PBP2 (Fig. 4A, S2B). This is interesting because while A22 and mec do not share the same protein target, MreB, the target of A22 directly interacts with PBP2, the target of mec, in the elongasome complex (van Teeffelen, Wang et al. 2011, Lee, Tropini et al. 2014, Morgenstein, Bratton et al. 2015). In addition, a similar phenotype has been reported for cephalexin treatment based off of an observation that a 1:100 dilution of cells is resistant to cephalexin while a 1:1000 dilution of cells is sensitive (Chung, Yao et al. 2009). While attempting to replicate this experiment unsuccessfully, we noticed that the reported starting O.D. of the 1:100 dilution more closely resembled that of a 1:10 (Fig. S4A). In an effort to more closely replicate the published results, we repeated the experiment with a 1:10 dilution and saw that cells become resistant to cephalexin although there is very little growth. This suggests that the action of cephalexin is very sensitive to the number of mass doublings cells undergo, but is a separate phenomenon from the DDGR reported here.

To confirm that the DDGR observed from mecillinam treatment is due to specific inhibition of PBP2 we shifted a temperature sensitive mutant of PBP2 (PBP2ts) to the nonpermissive temperature (40^{o} C) at different densities (Fig. 4C). Similar to A22 and mec addition, we found a density dependency on growth, as cells shifted at higher densities continue to grow better after the temperature shift. These data suggest that the elongasome is less essential at specific cell densities while overall PG synthesis remains essential. Another essential elongasome component is RodA, the transglycosylase partner

of PBP2 (Cho, Wivagg et al. 2016, Meeske, Riley et al. 2016). Similar to PBP2, a RodAts mutant displays better growth in restrictive temperatures at higher cell densities.

When mec was first developed in 1972, most experiments focused on efficacy and method of action (Lund and Tybring 1972, Melchior 1975, Spratt 1977). Mec's narrow target range allowed for precise exploration of the elongasome leading to the discovery of the Mre family of proteins (Wachi, Doi et al. 1987). Some researchers observed differences in cell survival to mecillinam based on density; however, to the best of our knowledge no mechanism has ever been put forth (Matsuhashi, Kamiryo et al. 1974, Spratt 1977). In the section below, we outline a possible mechanism for cell survival after A22 or mecillinam treatment.

PBP1B is needed for density-dependent growth resistance

The addition of A22 and mec at later time points does not reduce the growth rate of cells but does result in cells becoming round, indicating A22 and mecillinam are still able to inhibit their targets. These round cells continue to grow, both at the population level (O.D.) and single cell level (cell area) but do not lyse like cells treated with A22 at earlier time points (Fig. 1), suggesting a possible role for another PG synthase. Only deletion of PBP1B leads to the inhibition of DDGR for both A22 and mec, suggesting that PBP1B compensates for the loss of the elongasome in a density-dependent manner, and further refuting the idea that these specific antibiotics are being diluted out by increased cell numbers (Fig. 5AB).

PBP1A and PBP1B are aPBPs capable of performing both transglycoyslase and transpeptidase activities and have been shown to work independently from the MreB

based elongasome (Cho, Wivagg et al. 2016). It has been suggested that PBP1B is involved in division while PBP1A is involved in elongation (Cho, Wivagg et al. 2016, Ranjit, Jorgenson et al. 2017). Why and how PBP1B and the divisome alter activity in a cell density-dependent manner is unclear. While PBP1A and PBP1B can compensate for each other, PBP1B does have distinct functionality from PBP1A. PBP1B's transglycosylase domain is essential for de novo PG synthesis, while PBP1A is unable to perform de novo PG synthesis (Sarkar, Dutta et al. 2012, Ranjit, Jorgenson et al. 2017, Thulin and Andersson 2019). Interestingly, While PBP1B is mostly known for its role in the divisome there have been links to a role in the elongasome via A22 and mec sensitivity (Nichols, Sen et al. 2011, Barton, Grinnell et al. 2021). Additionally, our work shows PBP1B is necessary to overcome loss of PBP2 and MreB in a density-dependent manner as ΔPBP1B cells lyse when treated with mec or A22 (Fig. 5AB). It is possible that PBP1B is playing some role in linking elongasome and divisome activity.

DDGR has healthcare implications

The ability of bacteria to evade killing from antibiotics is an important clinical feature. In addition to being resistant to the effects of an antibiotic, which results in a higher MIC and is caused by heritable mutations, cells can avoid being killed through biofilm formation, antibiotic tolerance, and the formation of persister cells. Biofilms act as a physical barrier to block the diffusion of antibiotics keeping them away from the cell (Trampari, Holden et al. 2021). Tolerance and persistence both temporarily avoid cell death either by modifying growth rate or forming a metabolically inactive subpopulation (Brauner, Fridman et al. 2016, Harms, Maisonneuve et al. 2016). All three of these avoidance mechanisms can lead to mutations that eventually result in the accumulation of

resistance. Here, we show that DDGR is another method for bacteria to evade the effects of antibiotics.

The cell wall has always been an attractive antibiotic target due to its universality in bacteria and the lack of a PG cell wall in eukaryotic cells. Most Gram-negative rod-shaped pathogens utilize a Mre/Rod family-based cell wall synthesis system (Alyahya, Alexander et al. 2009) and therefore might display DDGR. The rod-shaped pathogens, *Pseudomonas aeruginosa* and *Shigella flexneri*, display DDGR in response to A22 (Fig. 6).

Grow in the presence of antibiotics due to DDGR can potentially allow cells to develop true resistance to antibiotics. Antibiotic cocktails have been long used as a method of treatment in antibiotic resistant infections (Rahal 1978, Yourassowsky, van der Linden et al. 1986). One complication of cocktails is that a higher number of drugs included in the cocktail the increases the likelihood of complex interactions, thereby making them less effective (Rahal 1978, Tekin, White et al. 2018). As best practice, drug cocktails should be kept to the minimum number of antibiotics needed to avoid these interactions and to minimize creating a super-resistant infection (Tekin, White et al. 2018). Simultaneous disruption of the elongasome and divisome, as seen in the cefsulodin-A22 or the cephalexin-A22 treated cells (Fig. 5D), is a way of overcoming DDGR. A cocktail of mecillinam, a clinically approved antibiotic for use in humans that is not currently widely used, and cefsulodin or cephalexin could increase the efficacy of both while only using two antibiotics and minimizing drug interactions.

Materials and Methods

Growth conditions

Overnight cultures were grown at 37ºC in a shaking incubator in Luria Bertani (LB) broth (Fisher Scientific: 244620) or MOPS (Teknova: M2106) supplemented with 0.2% glycerol. For growth curves a 1:1000 subculture of the overnight culture was made into fresh media and cells were grown shaking at 37ºC, unless otherwise noted. O.D.600 samples were taken every hour for the first two hours and then every 30 minutes. In cases of increased starting inoculum uninoculated media was removed so that all flasks had the same starting volume.

Slow growth conditions

MG1655 cells were inoculated 1:1000 from an overnight culture grown at 37ºC into LB and grown at 30ºC. O.D.600 measurements were taken every hour for the first two hours and then every 30 minutes. Slow growth was tested by inoculating MG1655 cells 1:1000 from an overnight culture, grown in M63 lactose media (M63 salts + casamino acids + 0.25% lactose) into fresh M63 lactose media. Measurements were taken once every hour for two hours before switching to measurements every 30 minutes. A22 (10 µg/ml) was added at the start of the growth curves or when cells reached an O.D.600 ~0.1.

Spent media testing

Overnight spent media was created by growing wild type cells in LB either overnight or to an O.D.600 ~0.1. 5 ml of overnight culture was spun down at 5000 x g for

10 minutes before filter (0.22µm) sterilization. The O.D.600 0.1 spent media was only filter sterilized. Overnight spent LB was mixed with fresh LB of the same batch to a final concentration of 10% before inoculation. 100% of the 0.1 spent LB was used. Cells were inoculated 1:1000 from an overnight culture of MG1655 cells. Both fresh LB and spent LB had A22 (10 µg/ml) added at the start of the growth curve and when the O.D.600 ~0.1. O.D.600 measurements were taken once every hour for two hours before switching to measurements every 30 minutes.

Increased cell density growth

Overnight cultures of MG1655 cells grown in LB were subcultured in 1:1000, 1:100, and 1:10 ratios into fresh LB. Cells were grown with and without A22 (10 µg/ml). $O.D._{600}$ measurements were taken every hour for two hours before measuring every 30 minutes.

Overnight cultures of MG1655 cells were grown in MOPS (0.2% glycerol) before being spun down and resuspended in fresh MOPS (0.2% glycerol). The $O.D._{600}$ was measured and this was then used to calculate the amount of culture needed for a starting $O.D._{600}$ of 0.1, 0.05, 0.025, and 0.0125 with the same final volume. Each starting $O.D._{600}$ condition was grown in LB or LB + A22 (10 µg/ml). $O.D._{600}$ measurements were then taken every 30 minutes.

Growth rates were calculated using the following formula $\text{Growth rate} = \frac{\log(O.D._{600}\ T2) - \log(O.D._{600}\ T2)}{0.301(\text{Hr})}$. Time points were chosen based on log phase (linear growth on a log-scale plot) and at least 30 minutes after exposure to A22 (10 µg/ml). In order to

average growth rates taken on different days we used the growth ratios $\frac{\text{Growth rate A22}}{\text{Growth rate control}}$ from each day and averaged across three days.

Growth stage testing

Sterile LB was kept at 37ºC and a culture of exponentially growing MG1655 cells at O.D.600 ~0.1 were subcultured into the pre-warmed media with and without A22 (10 µg/ml). The cells were diluted at 1:1, 1:10, and 1:100. O.D.600 measurements were taken every half hour post subculturing into pre-warmed media.

Temperature shift

Overnight cultures of MG1655 cells and LMC582 (PBPts), grown at 30ºC, cells were subcultured 1:1000 into flasks with LB +0.2% glycerol. Control flasks of each strain were kept at either 40ºC or 30ºC and not shifted over the course of the growth curve. Flasks was moved from the permissive to the non-permissive temperature every hour. $O.D._{600}$ measurements were taken every hour for two hours after which measurements were taken every 30 minutes.

Growth rates were calculated using the following formula $\text{Growth rate} = \frac{\log(O.D._{600}\ T2) - \log(O.D._{600}\ T2)}{0.301(\text{Hr})}$. Time points were chosen based on log phase and at least 30 minutes after temperature shift. In order to average growth rates taken on different days we used growth ratios $\frac{\text{Growth rate at 30ºC}}{\text{Growth rate at 40ºC}}$ and averaged across three days. Because cells shifted at T1 and T2 were shifted before reaching exponental growth we used the 30ºC control growth rates.

Deletion strains

All deletions were made via P1 lysate transduction from Keio deletion strains into MG1655 background. Transductants were selected on kanamycin plates and deletions were verified by PCR confirmation.

Microscopy

Growth conditions: MG1655 cells were diluted 1:1000 from and overnight culture in fresh LB at 37ºC. Cells treated with A22 (10 µg/ml) had the antibiotic added at 1 hour of growth. These cells were imaged at 1 hour of growth, 3 hours of growth, and 5 hours of growth. In a separate experiment cells were grown for 3 hours when A22 (10µg/ml) or mecillinam (3µg/ml) was added to the media. These cells were then imaged at 3 hours, 4 hours, and 6 hours.

Image acquisition: All imaging was done on M63 glucose 1% agarose pads at room temperature. Heat killed cells were placed in a boiling water bath for 10 minutes prior imaging. Phase contrast images were collected on a Nikon Ni-E epifluorescent microscope equipped with a 100X/1.45 NA objective (Nikon), Zyla 4.2 plus cooled sCMOS camera (Andor), and NIS Elements software (Nikon).

Microscopy analysis

The coefficient of variation of intracellular diameter deviation and cell area (µm2) were determined in MATLAB program Morphometrics (Morgenstein, Bratton et al. 2015, Ursell, Lee et al. 2017). Statistical significance was determined via ANOVA and

Tukey's HSD. All group comparisons not marked not significant are significant to a P-value of 0.0001.

Keio library screen

Cells were grown in 96-well plates from Keio deletion library plates. Overnight plate cultures were inoculated 1:100 into LB plates and A22 (1 µg/ml) plates and grown overnight. The ratio of LB O.D.600 and A22 O.D.600 were averaged across three repetitions and those strains with a ratio of 4 or higher were considered to be more sensitive to A22.

Starting $O.D._{600}$	A22 Growth Rate/MOPS Growth Rate	SD	P-value vs 0.1	P-value vs .05
0.1	0.999	0.0345	Na	0.851
0.05	0.956	0.0391	0.851	Na
0.025	0.800	0.1200	**0.025**	0.078
0.0125	0.691	0.0171	**0.002**	**0.005**

Table 1. **Increased cell density allows cells to grow in A22**. Growth rate ratio of cells in grown in A22 (10 μg/ml) vs MOPS. Students t-test to compare starting $O.D._{600}$ 0.1 group vs all other starting $O.D._{600}$ groups and starting $O.D._{600}$ 0.05 group vs all other starting $O.D._{600}$ groups. SD = standard deviation.

E. coli strains

Strain Name	Relevant Genotype	Source
MG1655	F- lambda- *ilvG- rfb-50 rph-1*	*E. coli* Genetic Stock Center
RS1	MG1655 *envC::kan*	This Study
RS2	MG1655 *yccK::kan*	This Study
LMC582	F- araD139 Δ(argF-lac)U169 deoC1 flbB5301 ptsF25 pbpa137(ts)	(Woldringh 1988)
LMC882	his, purB, proA, thi, lacY, rpsL, rodA(Ts)-52, zbe::Tn10	(Matsuzawa, Hayakawa et al. 1973)
ΔPBP1B	MG1655 *mrcB::kan*	This Study
ΔPBP1A	MG1655 *mrcA::kan*	This Study

P. aeruginosa strains

Strain Name	Relevant Genotype	Source
PA01	Wild Type	*Pseudomonas* Genetic Stock Center

S.Flexneri strains

Strain Name	Relevant Genotype	Source
ATCC 12022	Wild Type	ATCC

Table 2: *E. coli*, *P. aeruginosa*, and *S. flexneri* strains.

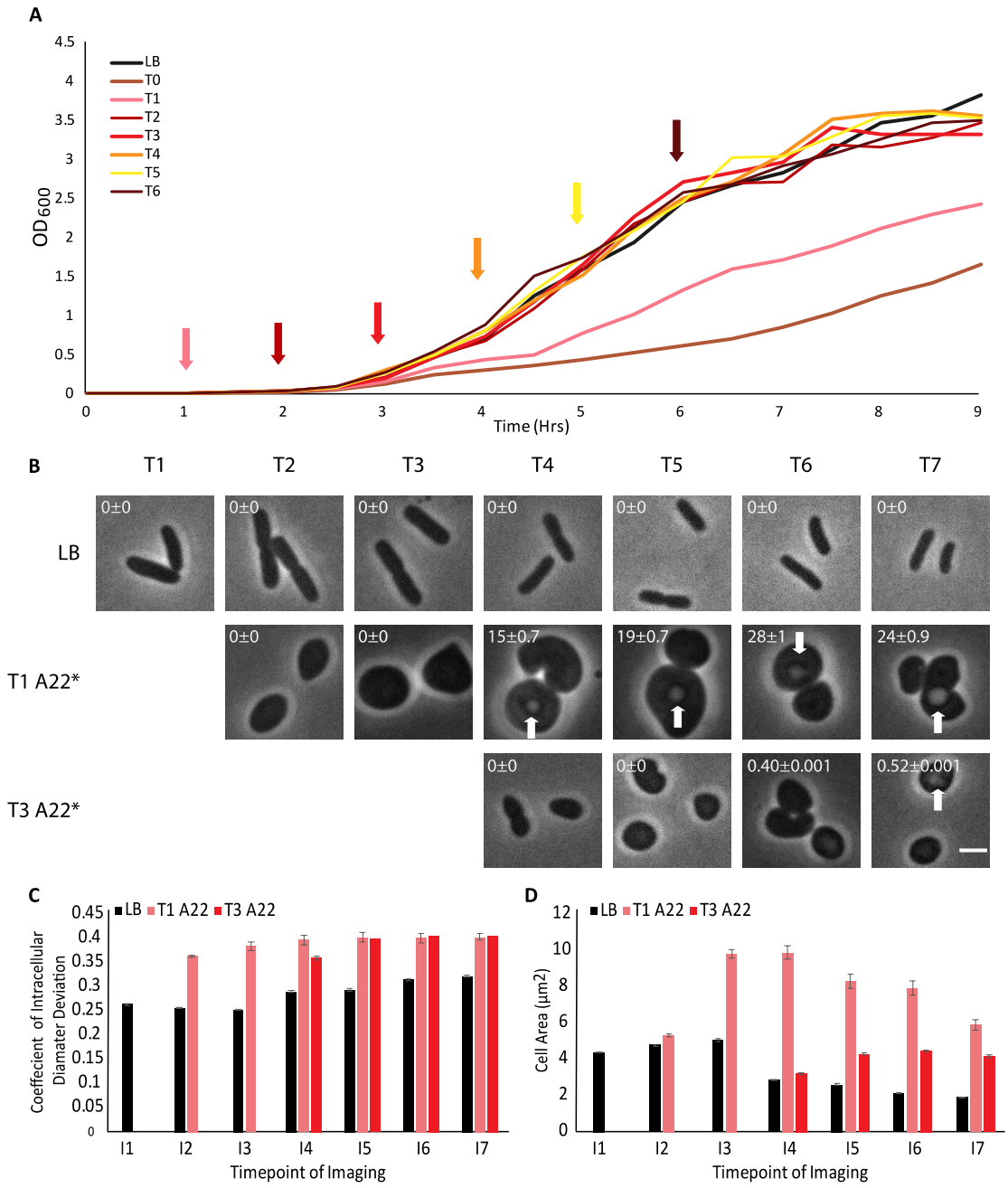

Figure 1. **Timing of A22 addition is important for growth rate changes.** (A) Representative growth curve of WT cells with A22 (10 µg/ml) added every hour from 0 to 6 hours as indicated by corresponding arrows. (B) Representative phase-contrast images of WT cells grown in LB, LB with A22 (10 µg/ml) added at one hour of growth, and LB with A22 added at 3 hours at growth. Cells were imaged every hour for seven hours. White arrow indicates cell vesicles forming in advance of lysis and numbers in the upper left represent percentage of cells displaying vesicles and the Poisson error to one standard deviation. Scale bar is equal to 2 µm. (C, D) Quantification of cells imaged in B.

Error bars are 95% CI. Data was pooled from three independent experiments. Numbers above the bars indicated total number of cells measured. (C) Coefficient of intracellular diameter deviation from cell imaging in B. (D) Cell area from cell imaging in B.

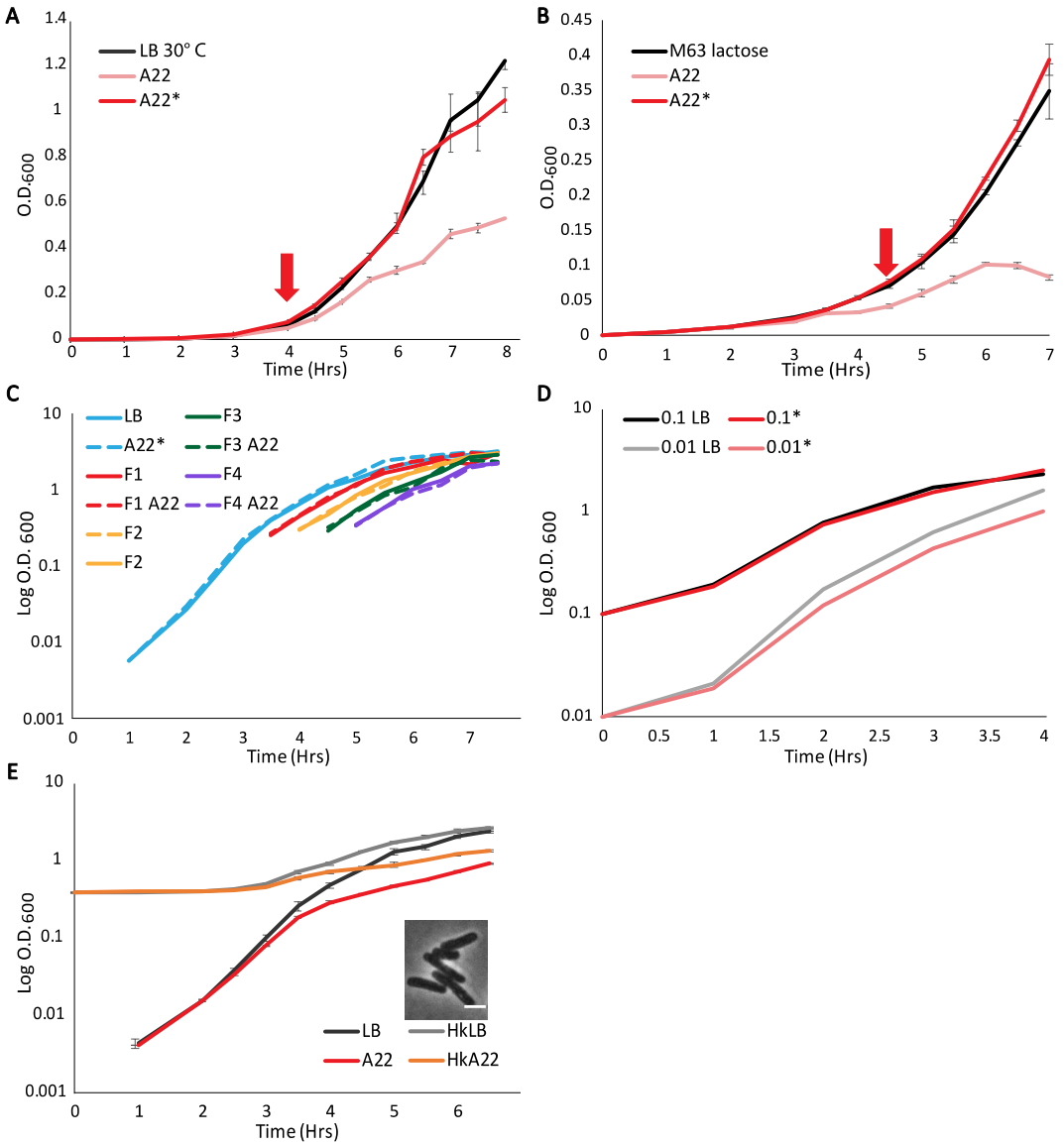

Figure 2. **Density dependent growth resistance is not caused by slow growth or limited mass doublings** (A) Growth curve of WT cells grown at 30° C in LB without A22, LB_{A22} (10 µg/ml), and A22 added at the indicated time where O.D.600 ~0.1 (*). (B) Growth curve of WT cells in M63 lactose media grown in LB, LB_{A22} (10 µg/ml), and A22 added at the indicated time where $O.D._{600}$ ~0.1 (*). (C) Representative growth curve of WT cells. Cells were grown for three hours and spiked with A22 (10 µg/ml) then inoculated at a 1:1 ratio into prewarmed LB and LB_{A22}(F1 and F1 A22). These cells were then grown for half an hour before repeating this procedure three more times. (F2-F4).

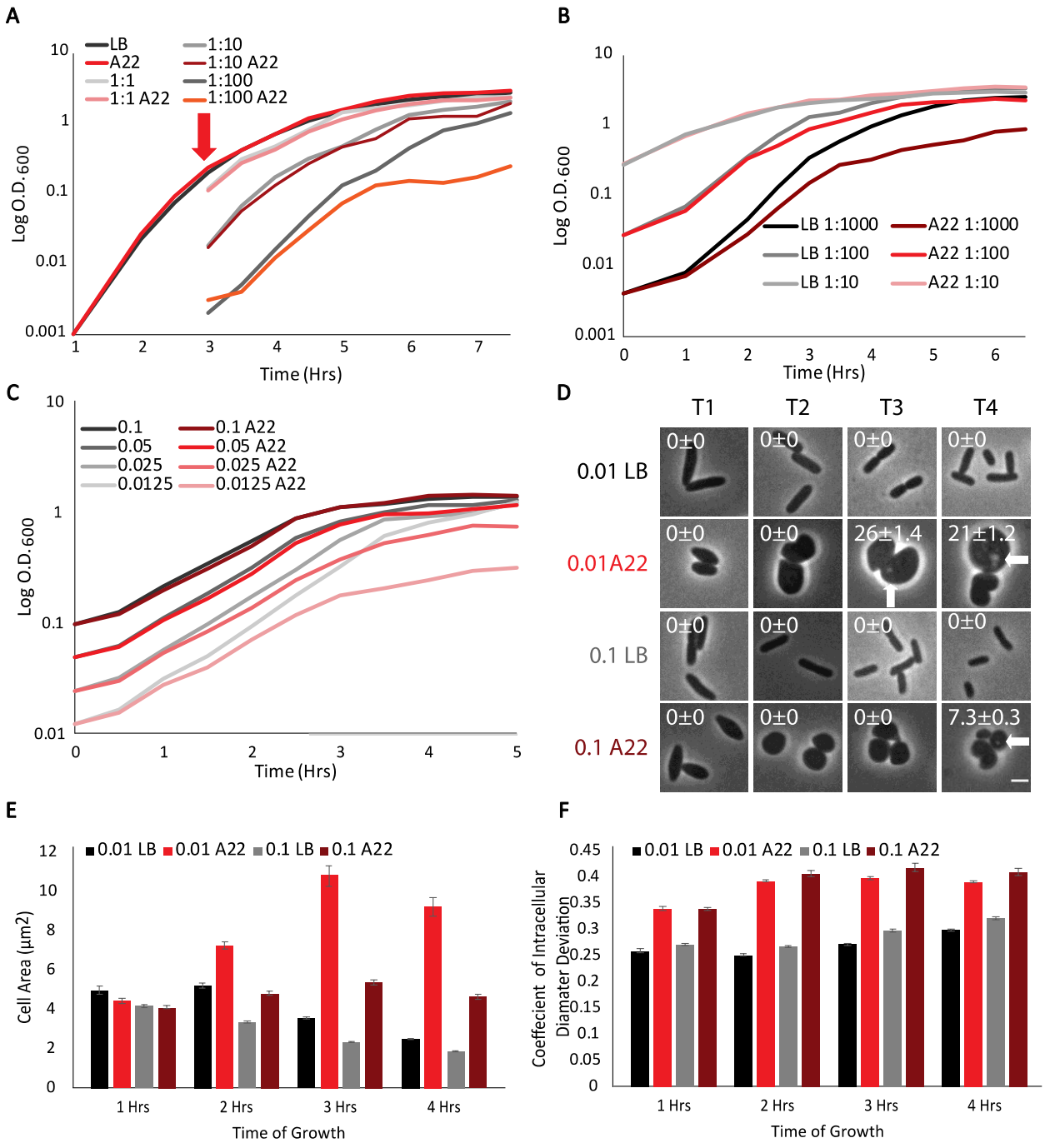

Figure 3. **Growth resistance is dependent on cell density.** (A) Representative log-scale growth curve of WT cells treated with A22. Cells were grown without A22 for three hours (arrow) and then either allowed to continue to grow, spiked with A22, or back-diluted into prewarmed media with and without A22 (10 µg/ml) at the indicated dilution factors. (B) Representative log-scale growth curve of wild type cells with different inoculation dilutions. Cells were grown with and without A22 (10 µg/ml) at the indicated initial inoculation ratio from overnight cells. (C) Representative log-scale growth curve of wild type cells with different starting O.D.s. Overnight cells were washed and

resuspended into new MOPS media and inoculated at the indicated $O.D._{600}$ with and without A22 (10 μg/ml). (D) Representative phase contrast images of WT cells grown from $O.D._{600}$~0.01 or 0.1 with and without A22 (10 μg/ml). Cells were imaged every hour for four hours. White arrow indicates cell vesicles forming in advance of lysis and numbers in the upper left represent percentage of cells displaying vesicles and the Poisson error to one standard deviation. Scale bar is equal to 2 μm. (E F) Quantification of cells imaged in D. Error bars are 95% CI. Data was pooled from three independent experiments. Numbers above the bars indicated total number of cells measured. (E) Cell area from cell imaging in D. (F) Coefficient of intracellular diameter deviation from cell imaging in D.

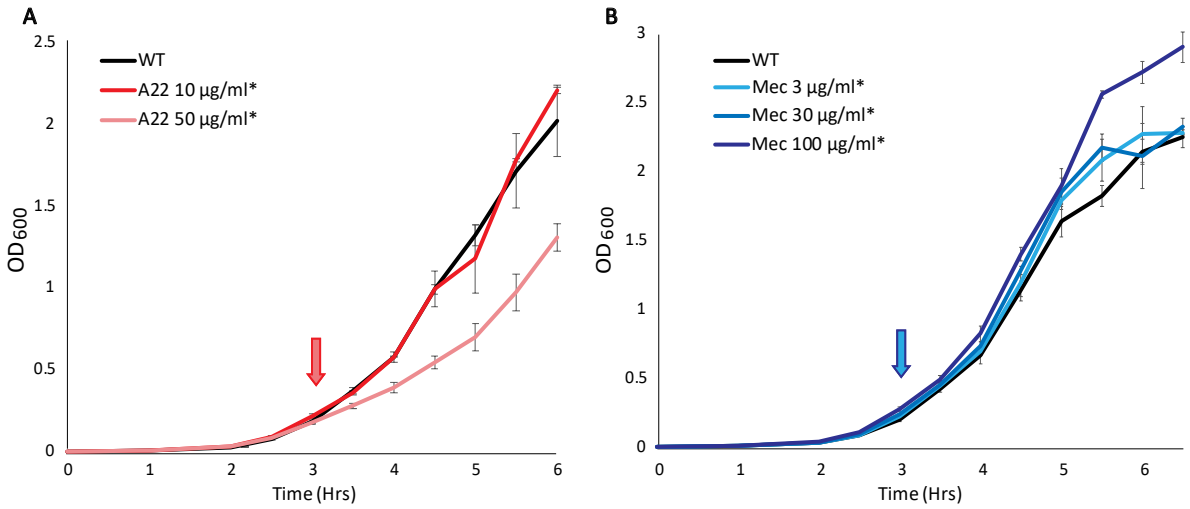

Figure 4. **Increased drug concentrations do not remove DDGR**. (A) Growth curve of WT cells grown without A22, A22 (10 µg/ml) added at the indicated time, and A22 (50 µg/ml) added at the indicated time where $O.D._{600}$ ~0.1 (*). (B) Growth curve of wild type cells. Grown without mecillinam, mecillinam (3 µg/ml) added at the indicated time where $O.D._{600}$ ~0.1, mecillinam (30 µg/ml) added at the indicated time where $O.D._{600}$ ~0.1, and mecillinam (100 µg/ml) added at the indicated time where $O.D._{600}$ ~0.1 (*).

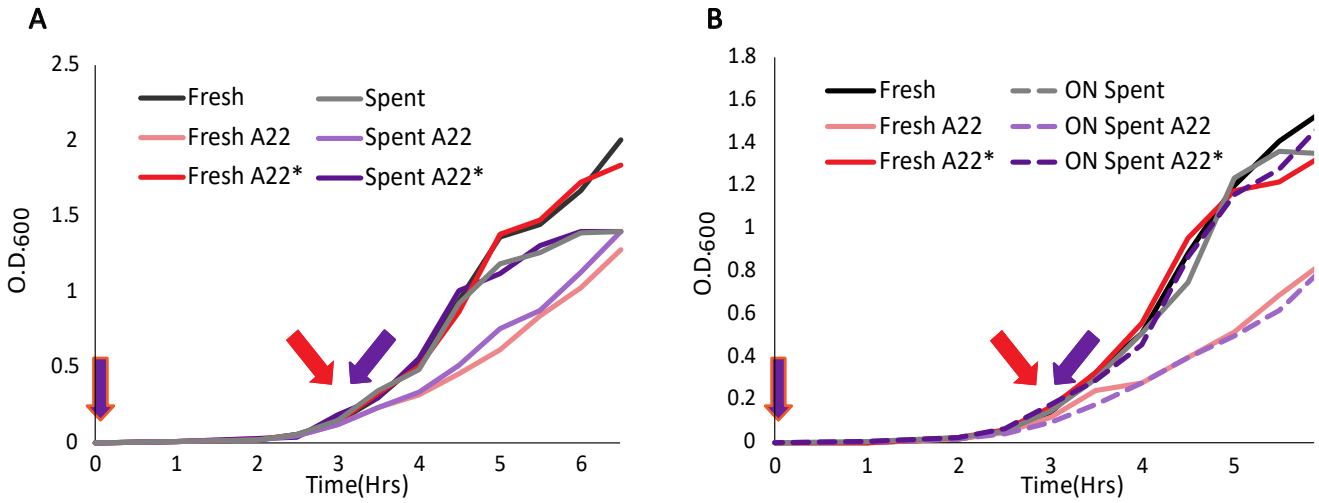

Figure 5. **Changes in media do not cause growth resistance.** Arrows are color coded to the lines representing spike (*) conditions. (A) Representative growth curve of WT cells with 100% spent media from a culture grown to an $O.D._{600}$ 0.1. Cells were grown in LB, A22 (10 μg/ml), and A22 added at the indicated time where $O.D._{600}$ ~0.1 (*). (B) Representative growth curve of WT cells with 10% spent media from an overnight culture. Cells were grown in LB, A22 (10 μg/ml), and A22 added at the indicated time where $O.D._{600}$ ~0.1 (*).

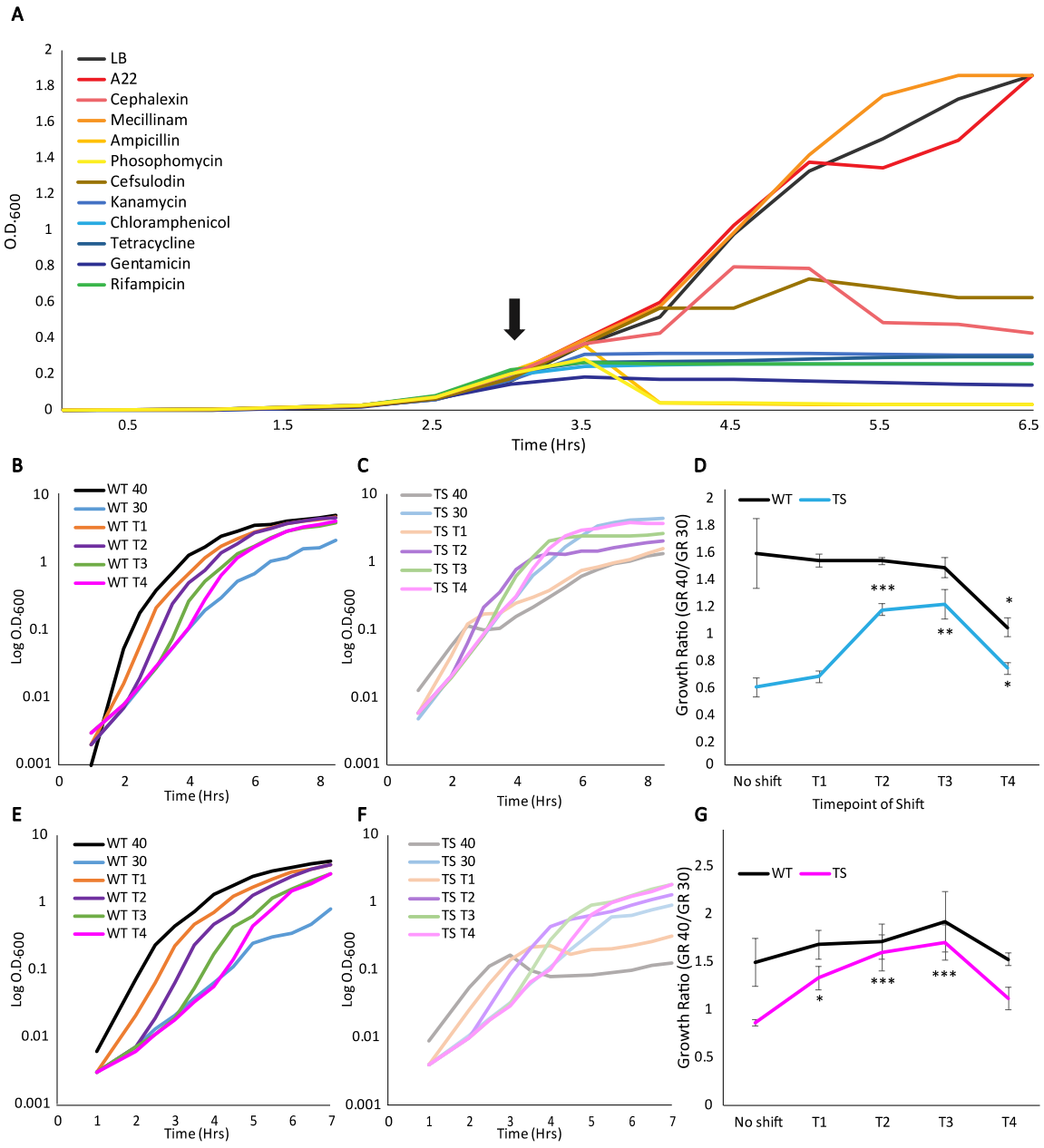

Figure 6. **PBP2 disruption also demonstrates growth resistance.** (A) Representative growth curve of WT cells treated with a variety of antibiotics at the indicated time (arrow). A22 (10 µg/ml), cephalexin (10 µg/ml), mecillinam (3 µg/ml), ampicillin (100 µg/ml), phosphomycin (10 µg/ml), cefsulodin (30 µg/ml), kanamycin (30 µg/ml), chloramphenicol (35 µg/ml), tetracycline (10 µg/ml), gentamycin (45 µg/ml), and rifampicin (500 µg/ml). (B) Representative growth curve of WT cells grown at 40ºC, 30º C, and shifted from 30º C to 40º C every hour every hour for four hours. (C) Representative growth curve of PBP2ts cells grown at 40ºC, 30º C, and shifted from 30º C to 40º C every hour every hour for four hours. (D) Pooled average growth rate ratios (growth rate at 40º C/growth rate at 30º C) from WT and PBP2ts. Cells were grown at 30º C and transferred to 40º C every hour for four hours. (E) Representative growth curve

of WT cells grown at 40ºC, 30º C, and shifted from 30º C to 40º C every hour. (F) Representative growth curve of RodAts cells grown at 40ºC, 30º C, and shifted from 30º C to 40º C every hour for four hours. Pooled average growth rate ratios (growth rate at 40º C/growth rate at 30º C) from WT and RodAts. Cells were grown at 30º C and transferred to 40º C every hour for four hours.

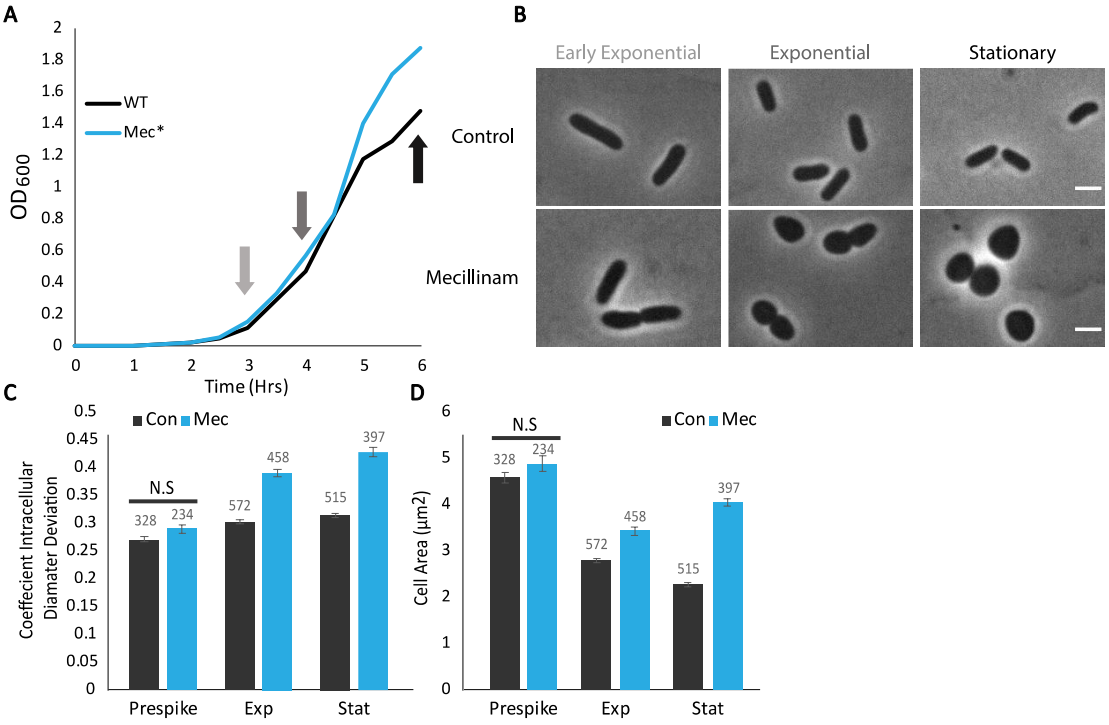

Figure 7. **Mecillinam is still active during DDGR** (A) Representative growth curve of WT cells used for imaging. Arrows indicate times used for imaging. Mecillinam (3 µg/ml) was added at the first arrow concurrently with imaging. (B) Representative phase contrast imaging of WT cells at early exponential phase, exponential phase, and stationary phase with and without A22 addition at early exponential phase. Scale bar is equal to 2µm. (C) Pooled coefficient of intracellular diameter deviation from cell imaging. All comparisons not marked not significant are statistically significant P <0.001. (D) Pooled cell area (μm^2) from cell imaging. All comparisons not marked not significant are statistically significant P <0.001.

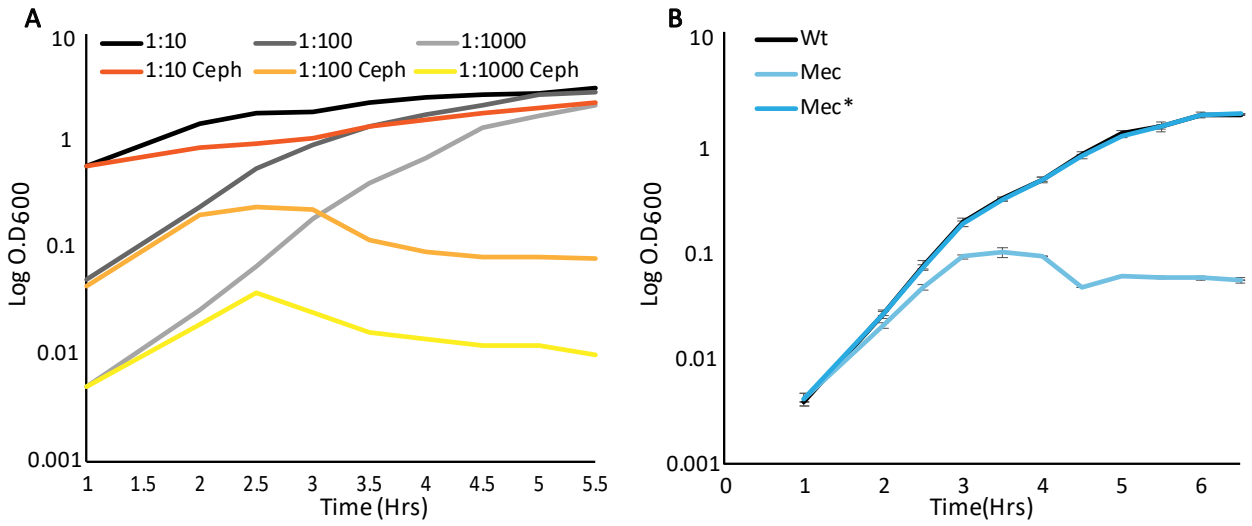

Figure 8. **Cephalexin does not display DDGR.** (A) Representative growth curve of WT cells grown in LB and $LB_{cephalexin}$ (10μg/ml) inoculated at the following ratios of overnight culture to new LB 1:10, 1:100, 1:1000. (B) Growth curve of WT cells grown in LB, $LB_{mecillinam}$ (3 μg/ml), and LB with mecillinam added at $O.D._{600}$ ~0.1 (T3).

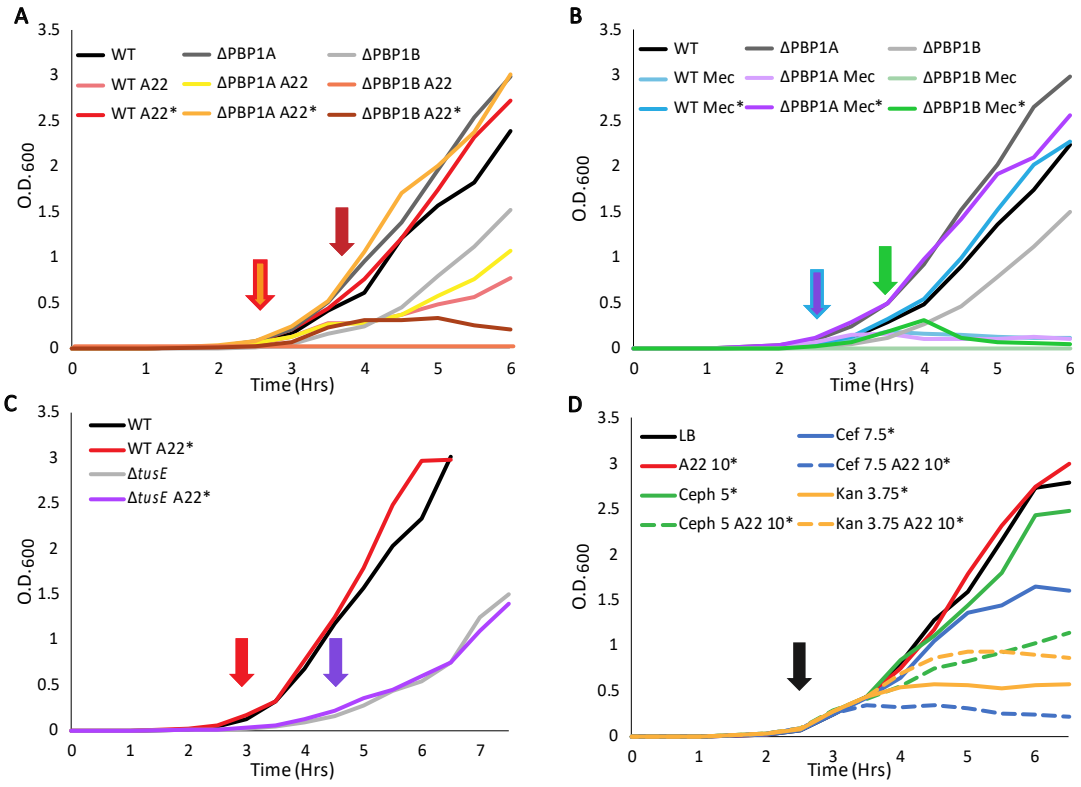

Figure 9. **PBP1B is necessary for density dependent growth resistance.** (A) Representative growth curve of WT, ΔPBP1A, and ΔPBP1B cells grown without A22, A22 (10 μg/ml), and A22 added at the indicated times where O.D.$_{600}$ ~0.1 (*). Arrow coloration corresponds to which strains were spiked at that time. (B) Representative growth curve of WT, ΔPBP1A, and ΔPBP1B grown without mecillinam, mecillinam (3 μg/ml), and mecillinam added at the indicated time per strain where O.D.$_{600}$~0.1. (*). (C) Representative growth curve of WT and *ΔtusE* grown without A22 and A22 (10 μg/ml) added at the indicated time per strain where O.D.$_{600}$~0.1. (*). (D) Representative growth curve of WT cells grown without antibiotics and the indicated antibiotics at the concentrations (μg/ml) added at the indicated time where O.D.$_{600}$ ~0.1 (arrow and *).

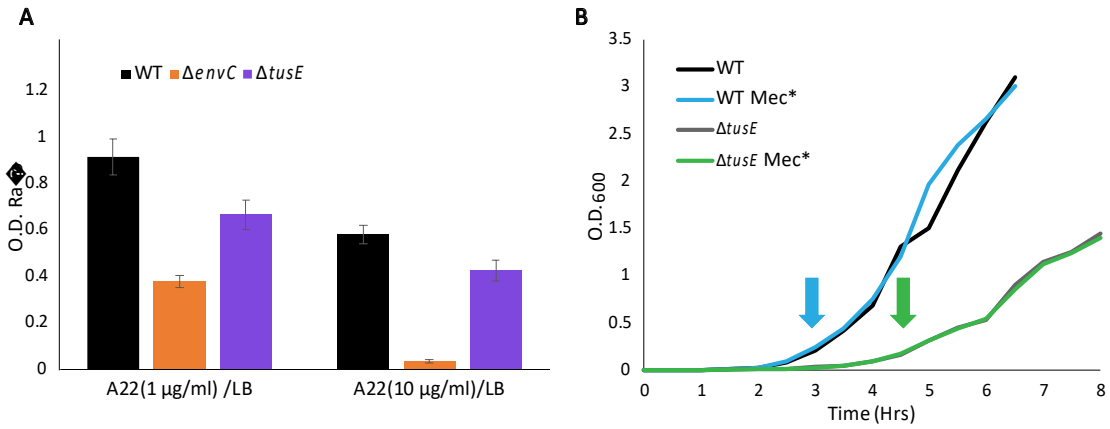

Figure 10. **Strain sensitive to A22 also display DDGR.** (A) Ratio of O.D.$_{600}$ of strains grown in 1 µg/ml or 10 µg/ml A22 vs LB for 6 hrs. (B) Representative growth curve of wild-type and Δ*tusE* strains. Grown without mecillinam, mecillinam (3 µg/ml), and mecillinam added at the indicated timepoint per strain where O.D.$_{600}$ ~0.1.

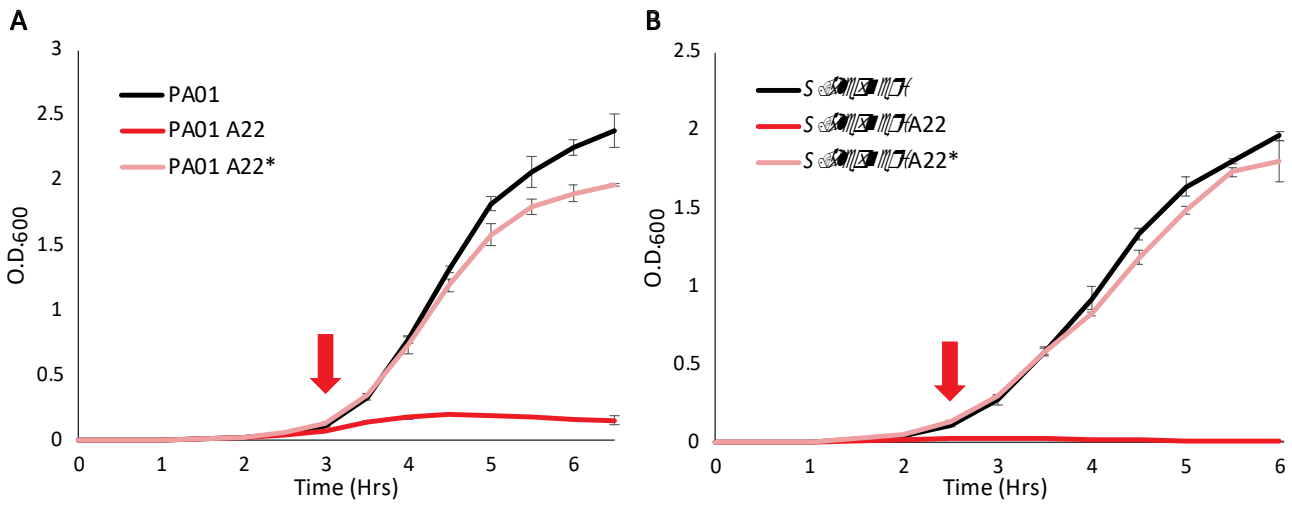

Figure 11. **Other Gram-negative rod species display DDGR.** (A) Growth curve of *Pseudomonas aeruginosa* PA01 in LB, LB_{A22} (20 µg/ml), and LB with A22 added at the indicated timepoint where $O.D._{600}$ ~0.1 (*). (B) Growth curve of *Shigella flexneri* (ATCC 12022) in LB, LB_{A22} (10 µg/ml), and LB with A22 added at the indicated timepoint where $O.D._{600}$ ~0.1 (*).

CHAPTER IV

DISCUSSION

Cell wall targeting antibiotics, particularly β-lactams, are used very commonly in clinical and laboratory settings. Two prominent reasons are that the cell wall is both essential for most bacteria making it an attractive target, and unique to bacteria, leading to a lack of cross reactivity in humans. β-lactams target the various penicillin binding proteins that synthesize the cell wall at the periplasmic stage. B-lactams prevent new wall growth by inhibiting transpeptidase activity and inducing breakdown of current cell wall, eventually leading to cell death (Zapun, Contreras-Martel et al. 2008, Worthington and Melander 2013, Cho, Uehara et al. 2014).

Other antibiotics target cell wall synthesis at different stages of PG synthesis, such as targeting lipid II in the membrane stage of synthesis or preventing the synthesis of glycan monomers in cytoplasmic stages (Sarkar, Yarlagadda et al. 2017). Because of the frequency of use during infections and the essentiality of the cell wall to bacteria, resistant mutants to these drugs occur frequently, methicillin resistant *Staphylococcus aureus* being a prominent example (Aminov and Mackie 2007, Davies and Davies 2010, Blair, Webber et al. 2015). Resistant mutations occur by chance or through horizontal gene transfer and are selected for in the presence of antibiotics. Any further chance for

resistant mutations comes from cells that can survive, even temporarily, leading to resistant strains and infections (Brauner, Fridman et al. 2016). MreB coordinates the activity and location of cylindrical cell wall synthesis in many bacilli and can be a good target for future antibiotics as it is essential for growth. A common lab-only antibiotic that targets MreB is A22, a thiourea derivative that depolymerizes MreB and prevents cell wall insertion in the cylinder of many bacilli (Bean, Flickinger et al. 2009). Unfortunately, A22 resistant mutants are regularly generated. Understanding reasons why this occurs and other methods for cells to develop resistance to A22 is key for any future clinical antibiotics targeting MreB.

Density-dependent growth resistance (DDGR) is the ability of rod cells to grow at wild-type (WT) rates post elongasome disruption in a manner dependent on cell density and independent from quorum sensing. So far, three essential components of the elongasome; MreB, RodA, and PBP2, have been shown to display DDGR. The dynamics of these three proteins is similar, implying they work together (Melchior 1975, Vijayan, Mallick et al. 2014, Morgenstein, Bratton et al. 2015). While DDGR allows for growth after inhibition of the elongasome the cells still display the characteristic round shape phenotype associated with disrupting these proteins (Melchior 1975, Bean, Flickinger et al. 2009). In addition, DDGR is transient as cells that display DDGR can lose it once subcultured to a lower cell density (Chapter III Fig. 3A). This implies that DDGR is not a form of resistance to antibiotics but rather a physiological change in the cell that modulates how deleterious of an effect these particular antibiotics can have. The closest comparison would be antibiotic tolerance. Tolerance is also transient but tends to apply to

antibiotics in general rather than only specific targets whereas DDGR only seems to occur specifically when only the elongasome is targeted (Windels, Michiels et al. 2019).

When cells are growing at higher density, they must be able to sense certain signals in order to measure and respond to the levels of nutrients and waste in addition to the number of cells around them. It appears there is a critical cell density that regardless of growth phase leads to a decrease in cell size (Chapter III Fig.1 BD and Fig. 3 DE). In both growth curves cells in LB reach a maximum cell size at an $O.D._{600} \sim 0.1$ before a significant decrease in size. It is possible that whatever causes this shift in cell size also protects the cells from the deleterious effects that begin to occur around the same time from A22 or mecillinam, a β-lactam specific to PBP2. The deleterious effect of A22 or mecillinam on growth and shape only becomes fully apparent after multiple rounds of division (Chapter III Fig. 1C and Fig. 3F). Smaller cell size is possibly linked to A22 resistance in external literature as FtsZ upregulated cells are both smaller than WT cells and also tolerant to A22 induced killing while still becoming round (Bendezú and de Boer 2008). While these experiments did not directly test whether smaller round cells are able to grow without a properly functioning elongasome, they suggest size may lead to protection. A22 induced death is preceded by intracellular vesicle formation; however, how small sphere cells might relate to less vesicle formation is not clear (Chapter III Fig. 1BD and Fig. 3DE). *ftsZ* expression is most likely not the cause of DDGR as it is expressed at a relatively constant level regardless of growth rate or density (Addinall and Holland 2002).

DDGR is not the only way that cell density has been linked to the lessened effects of antibiotics and exploring similar phenomena might lead to insights into the mechanism

of DDGR. The inoculum effect is an increase in the MIC when the starting inoculum amount is increased (Sabath, Garner et al. 1975). While β-lactams show the greatest increase in MIC due to the inoculum effect, the inoculum effect is considered to be present across all classes of antibiotics, whereas DDGR is not seen in all β-lactams nor across classes of antibiotics (Sabath, Garner et al. 1975, Lenhard and Bulman 2019). Although the mechanism behind the inoculum effect it is unknown, it is mainly used to describe variations in MIC as a laboratory phenomenon, but there is some discussion of its role in infection (Lenhard and Bulman 2019) (Udekwu, Parrish et al. 2009). A proposed mechanism for why β-lactams seem to most strongly display the inoculum effect is that PBPs are generally less expressed in stationary phase (Stevens, Van et al. 1993). I believe this explanation to be insufficient as inoculated cells are in lag phase independent of inoculum size and eventually exponential phase before they achieve stationary phase by the end of the assay, which would mean that the antibiotic would be effective again. There may still be some overlap in mechanism for both the inoculum effect and DDGR but there has been no work in this regard and the lack of DDGR in other β-lactams seems to indicate whatever overlap is small.

There are two main questions about DDGR for further exploration: what allows for continued growth of round cells, and how do cells sense density? While we implicate PBP1B as a necessary agent for DDGR and as serving a potential role in crosstalk between the elongasome and the divisome, it is unlikely to be the only protein necessary for round cell growth. PBP3, an essential divisome transpeptidase, is also probably necessary, but as an essential enzyme may be more difficulties to study (van der Ploeg, Verheul et al. 2013). Another protein implicated in resistance to mecillinam is SltY, a

lytic transglycosylase that breaks down glycan chains and is induced by β-lactams to breakdown the cell wall (Höltje, Mirelman et al. 1975, Cho, Uehara et al. 2014). An Δ*sltY* mutant displays DDGR for both A22 or mecillinam (Fig. 1) suggesting that either PG recycling or SltY specifically is not needed for growth after A22 treatment. There is a family of other lytic transglycosylases that may also play a role in round cell growth and PG recycling (van Heijenoort 2011). PG recycling must be important as DDGR is lost for mecillinam treatment in a strain that has PG recycling impaired (Cho, Uehara et al. 2014). The lack of PG recycling also leads to cells being more sensitive to A22 and having a reduced form of DDGR in response to (Fig. 2). It is possible that there may be redundancy between the lytic transglycosylases and a certain combination of lytic transglycosylases mutants will be needed to stop DDGR.

In order to come up with other potential proteins involved in DDGR, the transcriptional response to cells spiked with mecillinam and A22 were compared. RNA-seq was performed on cells grown in LB (control) or 1-hour post spike (O.D> 0.1) of $A22_{10}$, and $mecillinam_3$. When A22 or mecillinam spike cells were compared to the LB only control 55 genes were differentially regulated (Table 1). None of these genes have a direct role in cell wall synthesis; however, many of the genes in chemotaxis/flagella synthesis were upregulated as were genes involved in cysteine biosynthesis. Our lab has previously performed work showing that sublethal A22 treatment prevents chemotaxis but whether this relates to growth as a round cell is unexplored. Cysteine biosynthesis provides an unexpected but not unprecedented method of providing some level of protection from at least mecillinam. A previous study has shown cell lacking *cysB,* the transcriptional activator of cysteine biosynthesis, were more resistant to mecillinam

(Thulin and Andersson 2019). It is thought the reason Δ*cysB* cells are resistant to mecillinam is that they upregulate both PBP1B and LpoB, a lipoprotein that activates PBP1B (Thulin and Andersson 2019). We did not find PBP1B nor LpoB to be upregulated in our RNA-seq data. To determine the role of PBP1B LpoB and the additional PBP1B activators, DamX and DedD, will all be explored for roles in round cell growth and DDGR.

Arguably the more interesting question about DDGR is: how are cells detecting cell density without quorum sensing (QS)? The simplest possible explanation is that QS is occurring but that the signaling molecule is very short lived. Short lived QS would be plausible as our spent media was from overnight cultures; however, an $O.D._{600}$~0.5-0.1 is extremely low for canonical QS systems to be active (Wang, Liu et al. 2019). A second idea is that cell–cell contact is necessary and would occur, albeit briefly, even in a shaking liquid culture. Distinguishing between short lived QS and cell contact can be done by separating a high- and low-density culture with a semi-permeable membrane so that media is shared but cell-cell contact is inhibited between the two cultures. Growth of each culture would be measured in the presence of A22. Computer simulations of cell-cell contact in liquid could be informative to understand how the chance of cells contacting each other changes at different O.D.s to see if there is a large increase in probability at densities that DDGR is observed. Determining the mechanism of density sensing is only the first step into understanding DDGR. Next, it will be important to find the proteins necessary for relaying the density signal. We could use a transposon sequencing method to compare mutants from an A22 spike, mecillinam, mecillinam spike, or LB only condition. Transposon sequencing could have the benefit of selecting

against proteins needed for either density sensing or round cell growth. Separating these two may be difficult but it would allow us to include proteins of unknown function and all non-essential genes.

DDGR is a new and interesting phenomenon that allows cells to continue to grow in the presence of antibiotics potentially allowing for the accumulation of mutations leading to resistance. It is a narrow phenomenon only applying to the elongasome but seemingly to all of the elongasome. Further research into DDGR seems to offer new insight into how the proteins involved in the creation and maintenance of the cell wall interact with each and the wider cell's physiology. It also opens new questions into how the cell interacts with its environment and with other cells. DDGR may also give new insights into other similar density related reactions to antibiotics. DDGR is unlikely to be widely applicable in creating resistant strains but the methods in which DDGR can be overcome can also apply to other resistance mechanisms such as tolerance. DDGR and its study may be more useful overall as a direction for research into the cell wall and cell physiology, but that better understanding may eventually help in the fight against antibiotic resistance.

Strain Name	Relevant Genotype	Source
MG1655	F- lambda- *ilvG- rfb-50 rph-1*	*E. coli* Genetic Stock Center
Δ*sltY*	MG1655 *sltY::kan*	This study
Tu278	MG1655 *lacIZYA::frt lysA::frt ampD::frt*	(Cho, Uehara et al. 2014)

Table 3. ***E. coli* strain table**

ompF cmlB coa cry tolF b0929 JW0912	fliC flaF hag b1923 JW1908
ymgG b1172 JW5178	yebE b1846 JW1835
ycfJ b1110 JW1096	ycgR b1194 JW1183
flxA b1566 JW1558	cysU cysT b2424 JW2417
cysI b2763 JW2733	cysA b2422 JW2415
degP htrA ptd b0161 JW0157	amyA yedC b1927 JW1912
cysH b2762 JW2732	ygaC b2671 JW2646
ymgD b1171 JW5177	ynjH b1760 JW1749
bdm yddX b1481 JW5239	yecR b1904 JW1892
cysC b2750 JW2720	ypeC b2390 JW2387
cysJ b2764 JW2734	cheR cheX b1884 JW1873
fimI b4315 JW5779	fliD flaV flbC b1924 JW1909
cysN b2751 JW2721	fliS b1925 JW1910
fimC b4316 JW4279	ulaG yjfR b4192 JW5868
flhC flaI b1891 JW1880	ivy ykfE b0220 JW0210
spy b1743 JW1732	motB b1889 JW1878
fliT b1926 JW1911	yhjG yhjF b3524 JW3492
fimD b4317 JW5780	motA flaJ b1890 JW1879
cysD b2752 JW2722	yacC b0122 JW0118
ypfG b2466 JW2450	fcl wcaG yefB b2052 JW2037
fimA pilA b4314 JW4277	fimG b4319 JW4282
cysW b2423 JW2416	crfC yjdA b4109 JW4070
flhD flbB b1892 JW1881	ygaM b2672 JW2647
yaiY b0379 JW0370	ybhB b0773 JW0756

osmB b1283 JW1275	yehI b2118 JW2105
fimH b4320 JW4283	fimF b4318 JW4281
caiD yaaL b0036 JW0035	ubiK yqiC b3042 JW5505
ybgQ b0718 JW5099	

Table 4. **Genes with overlapping differential regulation in both A22 and mecillinam spikes.** A list of common gene names that were significantly different in the both mecillinam and A22 spikes compared to the control transcriptome.

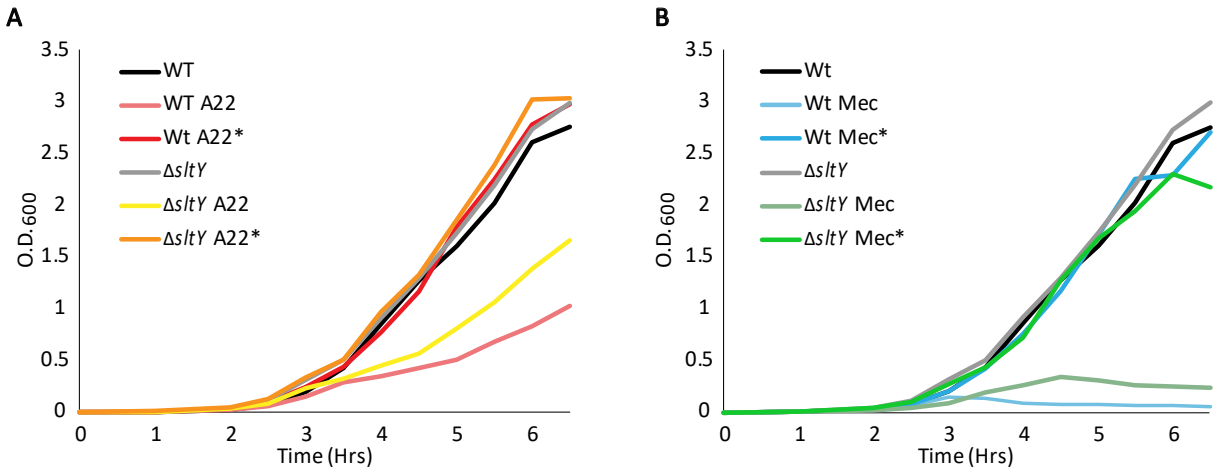

Figure 12. **SltY is not essential for DDGR.** (A) Representative growth curve of WT and Δ*sltY* cells grown without A22, A22 (10 μg/ml), and A22 added at T3 where $O.D._{600}$ ~0.1 (*). (B) Representative growth curve of WT and Δ*sltY* cells grown without mecillinam, mecillinam(3 μg/ml), and mecillinam added at T3 where $O.D._{600}$ ~0.1 (*).

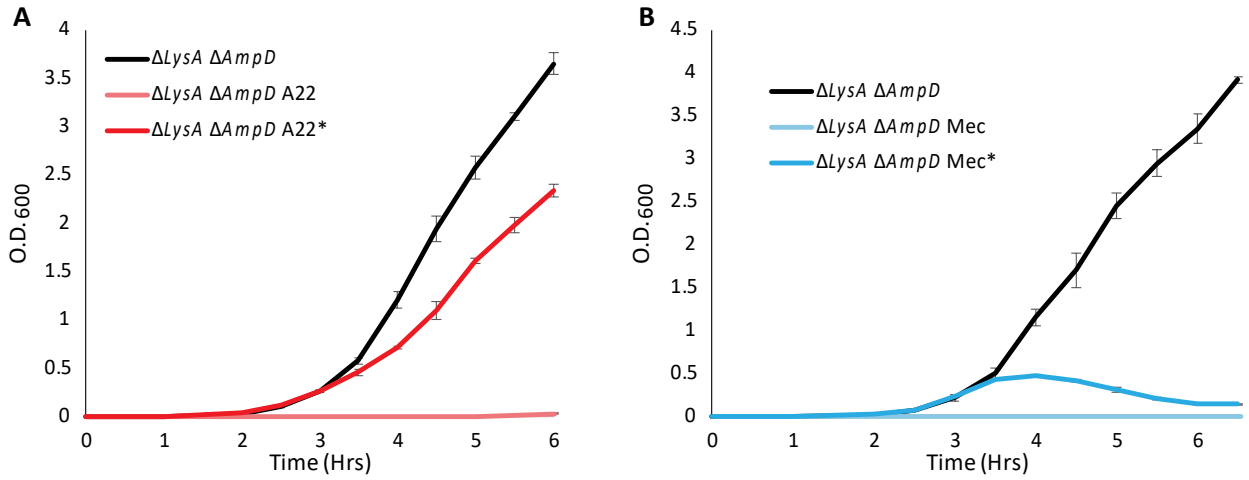

Figure 13. **Peptidoglycan recycling essential for mecillinam DDGR.** (A) Representative growth curve of WT and Δ*lysA* Δ*ampD* cells grown without A22, A22 (10 μg/ml), and A22 added at T3 where O.D.$_{600}$ ~0.1 (*). (B) Representative growth curve of WT and Δ*lysA* Δ*ampD* cells grown without mecillinam, mecillinam(3 μg/ml), and mecillinam added at T3 where O.D.$_{600}$ ~0.1 (*).

REFERENCES

Adams, D. W. and J. Errington (2009). "Bacterial cell division: assembly, maintenance and disassembly of the Z ring." Nature Reviews Microbiology **7**(9): 642-653.

Addinall, S. G. and B. Holland (2002). "The Tubulin Ancester, FtsZ, Draughtsman, Designer and Driving Force for Bacterial Cytokinesis." Journal of Molecular Biology **318**(2): 219-236.

Amato, S. M., C. H. Fazen, T. C. Henry, W. W. K. Mok, M. A. Orman, E. L. Sandvik, K. G. Volzing and M. P. Brynildsen (2014). "The role of metabolism in bacterial persistence." Frontiers in microbiology **5**: 70-70.

Aminov, R. I. and R. I. Mackie (2007). "Evolution and ecology of antibiotic resistance genes." FEMS Microbiology Letters **271**(2): 147-161.

Andrews, J. M. (2001). "Determination of minimum inhibitory concentrations." Journal of Antimicrobial Chemotherapy **48**(suppl_1): 5-16.

Ausmees, N., J. R. Kuhn and C. Jacobs-Wagner (2003). "The Bacterial Cytoskeleton: An Intermediate Filament-Like Function in Cell Shape." Cell **115**(6): 705-713.

Awuni, E. and Y. Mu (2019). "Effect of A22 on the Conformation of Bacterial Actin MreB." International Journal of Molecular Sciences **20**(6).

Balaban, N. Q., J. Merrin, R. Chait, L. Kowalik and S. Leibler (2004). "Bacterial Persistence as a Phenotypic Switch." Science **305**(5690): 1622.

Bartlett, T. M., B. P. Bratton, A. Duvshani, A. Miguel, Y. Sheng, N. R. Martin, J. P. Nguyen, A. Persat, S. M. Desmarais, M. S. VanNieuwenhze, K. C. Huang, J. Zhu, J. W. Shaevitz and Z. Gitai (2017). "A Periplasmic Polymer Curves *Vibrio cholerae* and Promotes Pathogenesis." Cell **168**(1-2): 172-185.e115.

Barton, B., A. Grinnell and R. M. Morgenstein (2021). "Disruption of the MreB Elongasome Is Overcome by Mutations in the Tricarboxylic Acid Cycle." Frontiers in Microbiology **12**: 970.

Bean, G. J., S. T. Flickinger, W. M. Westler, M. E. McCully, D. Sept, D. B. Weibel and K. J. Amann (2009). "A22 disrupts the bacterial actin cytoskeleton by directly binding and inducing a low-affinity state in MreB." Biochemistry **48**(22): 4852-4857.

Bendezú, F. O. and P. A. J. de Boer (2008). "Conditional Lethality, Division Defects, Membrane Involution, and Endocytosis in mre and mrd Shape Mutants of *Escherichia coli*." Journal of Bacteriology **190**(5): 1792.

Bigger, J. W. (1944). "Treatment of Staphyloeoeeal Infections with Penicillin by Intermittent Sterilisation." Lancet: 497-500.

Blair, J. M. A., M. A. Webber, A. J. Baylay, D. O. Ogbolu and L. J. V. Piddock (2015). "Molecular mechanisms of antibiotic resistance." Nature Reviews Microbiology **13**(1): 42-51.

Boniface, A., C. Parquet, M. Arthur, D. Mengin-Lecreulx and D. Blanot (2009). "The Elucidation of the Structure of *Thermotoga maritima* Peptidoglycan Reveals Two Novel Types of Cross-link*." Journal of Biological Chemistry **284**(33): 21856-21862.

Bratton, B. P., J. W. Shaevitz, Z. Gitai and R. M. Morgenstein (2018). "MreB polymers and curvature localization are enhanced by RodZ and predict *E. coli*'s cylindrical uniformity." Nature Communications **9**(1): 2797.

Brauner, A., O. Fridman, O. Gefen and N. Q. Balaban (2016). "Distinguishing between resistance, tolerance and persistence to antibiotic treatment." Nature Reviews Microbiology **14**(5): 320-330.
Breijyeh, Z., B. Jubeh and R. Karaman (2020). "Resistance of Gram-Negative Bacteria to Current Antibacterial Agents and Approaches to Resolve It." Molecules (Basel, Switzerland) **25**(6): 1340.
Brill, J., T. Hoffmann, M. Bleisteiner and E. Bremer (2011). "Osmotically controlled synthesis of the compatible solute proline is critical for cellular defense of *Bacillus subtilis* against high osmolarity." Journal of bacteriology **193**(19): 5335-5346.
Bui Nhat, K., J. Gray, H. Schwarz, P. Schumann, D. Blanot and W. Vollmer (2009). "The Peptidoglycan Sacculus of *Myxococcus xanthus* Has Unusual Structural Features and Is Degraded during Glycerol-Induced Myxospore Development." Journal of Bacteriology **191**(2): 494-505.
Cabeen, M. T., G. Charbon, W. Vollmer, P. Born, N. Ausmees, D. B. Weibel and C. Jacobs-Wagner (2009). "Bacterial cell curvature through mechanical control of cell growth." The EMBO journal **28**(9): 1208-1219.
Cava, F., M. A. de Pedro, H. Lam, B. M. Davis and M. K. Waldor (2011). "Distinct pathways for modification of the bacterial cell wall by non-canonical D-amino acids." The EMBO Journal **30**(16): 3442-3453.
Chattaway, F. W. (1982). "Microbial cell walls and membranes: by H J Rogers, H R Perkins and J B Ward. pp 564. Chapman & Hall, London. 1980 £30. ISBN 0-412-12030-5." Biochemical Education **10**(1): 33-33.
Cho, H., T. Uehara and T. G. Bernhardt (2014). "Beta-lactam antibiotics induce a lethal malfunctioning of the bacterial cell wall synthesis machinery." Cell **159**(6): 1300-1311.
Cho, H., C. N. Wivagg, M. Kapoor, Z. Barry, P. D. A. Rohs, H. Suh, J. A. Marto, E. C. Garner and T. G. Bernhardt (2016). "Bacterial cell wall biogenesis is mediated by SEDS and PBP polymerase families functioning semi-autonomously." Nature microbiology **1**: 16172-16172.
Colavin, A., H. Shi and K. Huang (2018). "RodZ modulates geometric localization of the bacterial actin MreB to regulate cell shape." Nature communications **9**: 1280.
Cooper, S. and M. W. Denny (1997). "A conjecture on the relationship of bacterial shape to motility in rod-shaped bacteria." FEMS Microbiology Letters **148**(2): 227-231.
Davies, J. and D. Davies (2010). "Origins and evolution of antibiotic resistance." Microbiology and molecular biology reviews : MMBR **74**(3): 417-433.
de Pedro, M. A., J. C. Quintela, J. V. Höltje and H. Schwarz (1997). "Murein segregation in *Escherichia coli*." Journal of bacteriology **179**(9): 2823-2834.
DeLisa, M. P. and W. E. Bentley (2002). "Bacterial autoinduction: looking outside the cell for new metabolic engineering targets." Microbial Cell Factories **1**(1): 5.
Depardieu, F., I. Podglajen, R. Leclercq, E. Collatz and P. Courvalin (2007). "Modes and modulations of antibiotic resistance gene expression." Clinical microbiology reviews **20**(1): 79-114.
Donlan, R. M. (2002). "Biofilms: microbial life on surfaces." Emerging infectious diseases **8**(9): 881-890.
Driehuis, F., B. de Jonge and N. Nanninga (1992). "Cross-linkage and cross-linking of peptidoglycan in *Escherichia coli*: definition, determination, and implications." Journal of bacteriology **174**(6): 2028-2031.
Dusenbery, D. B. (1998). "Fitness landscapes for effects of shape on chemotaxis and other behaviors of bacteria." Journal of bacteriology **180**(22): 5978-5983.
Espeli, O., P. Nurse, C. Levine, C. Lee and K. J. Marians (2003). "SetB: an integral membrane protein that affects chromosome segregation in Escherichia coli." Molecular Microbiology **50**(2): 495-509.
Esue, O., L. Rupprecht, S. X. Sun and D. Wirtz (2010). "Dynamics of the Bacterial Intermediate Filament Crescentin In Vitro and In Vivo." PLOS ONE **5**(1): e8855.

Ferrero, R. L. and A. Lee (1988). "Motility of *Campylobacter jejuni* in a viscous environment: comparison with conventional rod-shaped bacteria." Journal of General Microbiology(0022-1287 (Print)).
Freire, P., R. Neves Moreira and C. M. Arraiano (2009). "BolA Inhibits Cell Elongation and Regulates MreB Expression Levels." Journal of Molecular Biology **385**(5): 1345-1351.
Furchtgott, L., N. S. Wingreen and K. C. Huang (2011). "Mechanisms for maintaining cell shape in rod-shaped Gram-negative bacteria." Molecular microbiology **81**(2): 340-353.
García del Portillo, F. and M. A. de Pedro (1990). "Differential effect of mutational impairment of penicillin-binding proteins 1A and 1B on *Escherichia coli* strains harboring thermosensitive mutations in the cell division genes ftsA, ftsQ, ftsZ, and pbpB." Journal of bacteriology **172**(10): 5863-5870.
Gefen, O. and N. Q. Balaban (2009). "The importance of being persistent: heterogeneity of bacterial populations under antibiotic stress." FEMS Microbiology Reviews **33**(4): 704-717.
Handwerger, S. and A. Tomasz (1985). "Antibiotic Tolerance Among Clinical Isolates of Bacteria." Annual Review of Pharmacology and Toxicology **25**(1): 349-380.
Harms, A., E. Maisonneuve and K. Gerdes (2016). "Mechanisms of bacterial persistence during stress and antibiotic exposure." Science **354**(6318): aaf4268.
Hayhurst, E. J., L. Kailas, J. K. Hobbs and S. J. Foster (2008). "Cell wall peptidoglycan architecture in *Bacillus subtilis*." Proceedings of the National Academy of Sciences of the United States of America **105**(38): 14603-14608.
Heijenoort, J. v. (2001). "Formation of the glycan chains in the synthesis of bacterial peptidoglycan." Glycobiology **11**(3): 25R-36R.
Höltje, J. V., D. Mirelman, N. Sharon and U. Schwarz (1975). "Novel type of murein transglycosylase in Escherichia coli." Journal of bacteriology **124**(3): 1067-1076.
Huang, K. C., R. Mukhopadhyay, B. Wen, Z. Gitai and N. S. Wingreen (2008). "Cell shape and cell-wall organization in Gram-negative bacteria." Proceedings of the National Academy of Sciences **105**(49): 19282.
Hussain, S., C. N. Wivagg, P. Szwedziak, F. Wong, K. Schaefer, T. Izoré, L. D. Renner, M. J. Holmes, Y. Sun, A. W. Bisson-Filho, S. Walker, A. Amir, J. Löwe and E. C. Garner (2018). "MreB filaments align along greatest principal membrane curvature to orient cell wall synthesis." eLife **7**: e32471.
Joseleau-Petit, D., J.-C. Liébart, J. A. Ayala and R. D'Ari (2007). "Unstable *Escherichia coli* L forms revisited: growth requires peptidoglycan synthesis." Journal of bacteriology **189**(18): 6512-6520.
Kim, J.-S., R. Yamasaki, S. Song, W. Zhang and T. K. Wood (2018). "Single cell observations show persister cells wake based on ribosome content." Environmental Microbiology **20**(6): 2085-2098.
Kruse, T., J. Bork-Jensen and K. Gerdes (2005). "The morphogenetic MreBCD proteins of *Escherichia coli* form an essential membrane-bound complex." Molecular Microbiology **55**(1): 78-89.
Krzyżek, P. and G. Gościniak (2018). "Morphology of Helicobacter pylori as a result of peptidoglycan and cytoskeleton rearrangements." Przeglad gastroenterologiczny **13**(3): 182-195.
Kudo, S., N. Imai, M. Nishitoba, S. Sugiyama and Y. Magariyama (2005). "Asymmetric swimming pattern of *Vibrio alginolyticus* cells with single polar flagella." FEMS Microbiology Letters **242**(2): 221-225.
Kurita, K., F. Kato and D. Shiomi (2020). "Alteration of Membrane Fluidity or Phospholipid Composition Perturbs Rotation of MreB Complexes in *Escherichia coli*." Frontiers in Molecular Biosciences **7**: 364.
Kurita, K., R. Shin, T. Tabei and D. Shiomi (2019). "Relation between rotation of MreB actin and cell width of *Escherichia coli*." Genes to Cells **24**(3): 259-265.

Kvist, M., V. Hancock and P. Klemm (2008). "Inactivation of efflux pumps abolishes bacterial biofilm formation." Applied and environmental microbiology **74**(23): 7376-7382.
Lee, T. K., C. Tropini, J. Hsin, S. M. Desmarais, T. S. Ursell, E. Gong, Z. Gitai, R. D. Monds and K. C. Huang (2014). "A dynamically assembled cell wall synthesis machinery buffers cell growth." Proceedings of the National Academy of Sciences **111**(12): 4554.
Lenhard, J. R. and Z. P. Bulman (2019). "Inoculum effect of β-lactam antibiotics." Journal of Antimicrobial Chemotherapy **74**(10): 2825-2843.
Levin-Reisman, I., A. Brauner, I. Ronin and N. Q. Balaban (2019). "Epistasis between antibiotic tolerance, persistence, and resistance mutations." Proceedings of the National Academy of Sciences **116**(29): 14734.
Levinson, W. a. (2018). Review of Medical Microbiology & Immunology : A Guide to Clinical Infectious Diseases, 15e. New York, N.Y. :, McGraw-Hill Education LLC.
Li, X.-Z. and H. Nikaido (2004). "Efflux-Mediated Drug Resistance in Bacteria." Drugs **64**(2): 159-204.
Li, X.-Z. and H. Nikaido (2009). "Efflux-mediated drug resistance in bacteria: an update." Drugs **69**(12): 1555-1623.
Lin, T.-Y. and D. B. Weibel (2016). "Organization and function of anionic phospholipids in bacteria." Applied Microbiology and Biotechnology **100**(10): 4255-4267.
Liu, Y. and E. Breukink (2016). "The Membrane Steps of Bacterial Cell Wall Synthesis as Antibiotic Targets." Antibiotics (Basel, Switzerland) **5**(3): 28.
Lopatkin, A. J., J. M. Stokes, E. J. Zheng, J. H. Yang, M. K. Takahashi, L. You and J. J. Collins (2019). "Bacterial metabolic state more accurately predicts antibiotic lethality than growth rate." Nature microbiology **4**(12): 2109-2117.
Magariyama, Y., M. Ichiba, K. Nakata, K. Baba, T. Ohtani, S. Kudo and T. Goto (2005). "Difference in bacterial motion between forward and backward swimming caused by the wall effect." Biophysical journal **88**(5): 3648-3658.
Maki, N., J. E. Gestwicki, E. M. Lake, L. L. Kiessling and J. Adler (2000). "Motility and chemotaxis of filamentous cells of *Escherichia coli*." Journal of bacteriology **182**(15): 4337-4342.
Matsuzawa, H., K. Hayakawa, T. Sato and K. Imahori (1973). "Characterization and genetic analysis of a mutant of *Escherichia coli* K-12 with rounded morphology." Journal of bacteriology **115**(1): 436-442.
McDermott, W. (1958). "Microbial persistence." The Yale journal of biology and medicine **30**(4): 257-291.
McKinnon, P. S. and S. L. Davis (2004). "Pharmacokinetic and Pharmacodynamic Issues in the Treatment of Bacterial Infectious Diseases." European Journal of Clinical Microbiology and Infectious Diseases **23**(4): 271-288.
Melchior, L. T. a. N. H. (1975). "Mecillinam (FL 1060), a 6,3-Amidinopenicillanic Acid

Derivative: Bactericidal Action and Synergy In Vitro." Antimicrobial Agents and Chemotherapy **8**: 271-276.
Michiels, J. E., B. Van den Bergh, N. Verstraeten and J. Michiels (2016). "Molecular mechanisms and clinical implications of bacterial persistence." Drug Resistance Updates **29**: 76-89.
Mitchell, James G. (2002). "The Energetics and Scaling of Search Strategies in Bacteria." The American Naturalist **160**(6): 727-740.
Morgenstein, R. M., B. P. Bratton, J. P. Nguyen, N. Ouzounov, J. W. Shaevitz and Z. Gitai (2015). "RodZ links MreB to cell wall synthesis to mediate MreB rotation and robust morphogenesis." Proceedings of the National Academy of Sciences **112**(40): 12510.
Motaleb, M. A., L. Corum, J. L. Bono, A. F. Elias, P. Rosa, D. S. Samuels and N. W. Charon (2000). "*Borrelia burgdorferi* periplasmic flagella have both skeletal and motility functions." Proceedings of the National Academy of Sciences of the United States of America **97**(20): 10899-10904.

Nanninga, N. (1988). "Growth and form in microorganisms: morphogenesis of Escherichia coli." Canadian Journal of Microbiology **34**(4): 381-389.
Neu, H. C. (1985). "Infections Due to Gram-Negative Bacteria: An Overview." Reviews of Infectious Diseases **7**(Supplement_4): S778-S782.
Oswald, F., A. Varadarajan, H. Lill, E. J. G. Peterman and Y. J. M. Bollen (2016). "MreB-Dependent Organization of the *E. coli* Cytoplasmic Membrane Controls Membrane Protein Diffusion." Biophysical journal **110**(5): 1139-1149.
Persat, A., H. A. Stone and Z. Gitai (2014). "The curved shape of Caulobacter crescentus enhances surface colonization in flow." Nature communications **5**: 3824-3824.
Pisabarro, A. G., M. A. de Pedro and D. Vázquez (1985). "Structural modifications in the peptidoglycan of *Escherichia coli* associated with changes in the state of growth of the culture." Journal of bacteriology **161**(1): 238-242.
Pumbwe, L., C. A. Skilbeck and H. M. Wexler (2008). "Presence of Quorum-sensing Systems Associated with Multidrug Resistance and Biofilm Formation in *Bacteroides fragilis*." Microbial Ecology **56**(3): 412-419.
Quintela, J., M. Caparrós and M. A. de Pedro (1995). "Variability of peptidoglycan structural parameters in Gram-negative bacteria." FEMS Microbiology Letters **125**(1): 95-100.
Rajput, A., A. Thakur, S. Sharma and M. Kumar (2018). "aBiofilm: a resource of anti-biofilm agents and their potential implications in targeting antibiotic drug resistance." Nucleic acids research **46**(D1): D894-D900.
Rani, G. and I. Patri (2019). "The importance of being cross-linked for the bacterial cell wall." bioRxiv: 573113.
Robertson, B. R., J. L. Rourke, B. A. Neilan, P. Vandamme, S. L. W. On, J. G. Fox and A. Lee (2005). "*Mucispirillum schaedler*i gen. nov., sp. nov., a spiral-shaped bacterium colonizing the mucus layer of the gastrointestinal tract of laboratory rodents." International Journal of Systematic and Evolutionary Microbiology **55**(3): 1199-1204.
Sabath, L. D., C. Garner, C. Wilcox and M. Finland (1975). "Effect of inoculum and of beta-lactamase on the anti-staphylococcal activity of thirteen penicillins and cephalosporins." Antimicrobial agents and chemotherapy **8**(3): 344-349.
Salje, J., F. van den Ent, P. de Boer and J. Löwe (2011). "Direct Membrane Binding by Bacterial Actin MreB." Molecular Cell **43**(3): 478-487.
Santos, J. M., M. Lobo, A. P. A. Matos, M. A. De Pedro and C. M. Arraiano (2002). "The gene bolA regulates dacA (PBP5), dacC (PBP6) and ampC (AmpC), promoting normal morphology in *Escherichia coli*." Molecular Microbiology **45**(6): 1729-1740.
Sarkar, P., V. Yarlagadda, C. Ghosh and J. Haldar (2017). "A review on cell wall synthesis inhibitors with an emphasis on glycopeptide antibiotics." MedChemComm **8**(3): 516-533.
Schaechter, M., O. MaalØe and N. O. Kjeldgaard (1958). "Dependency on Medium and Temperature of Cell Size and Chemical Composition during Balanced Growth of Salmonella typhimurium." Microbiology **19**(3): 592-606.
Shaevitz, J. W. and Z. Gitai (2010). "The structure and function of bacterial actin homologs." Cold Spring Harbor perspectives in biology **2**(9): a000364-a000364.
Shiomi, D. (2017). "Polar localization of MreB actin is inhibited by anionic phospholipids in the rod-shaped bacterium Escherichia coli." Current Genetics **63**(5): 845-848.
Silversmith, R. E. and R. B. Bourret (1999). "Throwing the switch in bacterial chemotaxis." Trends in Microbiology **7**(1): 16-22.
Stevens, D. L., S. Van and A. E. Bryant (1993). "Penicillin-Binding Protein Expression at Different Growth Stages Determines Penicillin Efficacy In Vitro and In Vivo: An Explanation for the Inoculum Effect." The Journal of Infectious Diseases **167**(6): 1401-1405.
Strahl, H., F. Bürmann and L. W. Hamoen (2014). "The actin homologue MreB organizes the bacterial cell membrane." Nature Communications **5**(1): 3442.

Takeuchi, S., W. R. DiLuzio, D. B. Weibel and G. M. Whitesides (2005). "Controlling the shape of filamentous cells of *Escherichia coli*." Nano letters **5**(9): 1819-1823.
Thulin, E. and D. I. Andersson (2019). "Upregulation of PBP1B and LpoB in cysB Mutants Confers Mecillinam (Amdinocillin) Resistance in *Escherichia coli*." Antimicrobial agents and chemotherapy **63**(10): e00612-00619.
Trampari, E., E. R. Holden, G. J. Wickham, A. Ravi, L. d. O. Martins, G. M. Savva and M. A. Webber (2021). "Exposure of *Salmonella* biofilms to antibiotic concentrations rapidly selects resistance with collateral tradeoffs." npj Biofilms and Microbiomes **7**(1): 3.
Tuomanen, E., R. M. Cozens, W. Tosch, O. Zak and A. Tomasz (1986). "The Rate of Killing of *Escherichia coli* by Beta-Lactam Antibiotics is Strictly Proportional to the Rate of Bacterial Growth." Journal of general microbiology **132**: 1297-1304.
Turner, R. D., A. F. Hurd, A. Cadby, J. K. Hobbs and S. J. Foster (2013). "Cell wall elongation mode in Gram-negative bacteria is determined by peptidoglycan architecture." Nature communications **4**: 1496-1496.
Turner, R. D., S. Mesnage, J. K. Hobbs and S. J. Foster (2018). "Molecular imaging of glycan chains couples cell-wall polysaccharide architecture to bacterial cell morphology." Nature Communications **9**(1): 1263.
Turner, R. D., W. Vollmer and S. J. Foster (2014). "Different walls for rods and balls: the diversity of peptidoglycan." Molecular microbiology **91**(5): 862-874.
Udekwu, K. I., N. Parrish, P. Ankomah, F. Baquero and B. R. Levin (2009). "Functional relationship between bacterial cell density and the efficacy of antibiotics." The Journal of antimicrobial chemotherapy **63**(4): 745-757.
van den Ent, F., T. Izoré, T. A. Bharat, C. M. Johnson and J. Löwe (2014). "Bacterial actin MreB forms antiparallel double filaments." eLife **3**: e02634-e02634.
van der Ploeg, R., J. Verheul, N. O. E. Vischer, S. Alexeeva, E. Hoogendoorn, M. Postma, M. Banzhaf, W. Vollmer and T. den Blaauwen (2013). "Colocalization and interaction between elongasome and divisome during a preparative cell division phase in *Escherichia coli*." Molecular Microbiology **87**(5): 1074-1087.
van Heijenoort, J. (2011). "Peptidoglycan hydrolases of Escherichia coli." Microbiology and molecular biology reviews : MMBR **75**(4): 636-663.
van Teeffelen, S., S. Wang, L. Furchtgott, K. C. Huang, N. S. Wingreen, J. W. Shaevitz and Z. Gitai (2011). "The bacterial actin MreB rotates, and rotation depends on cell-wall assembly." Proceedings of the National Academy of Sciences **108**(38): 15822.
Varma, A. and K. D. Young (2009). "*Escherichia coli*, MreB and FtsZ Direct the Synthesis of Lateral Cell Wall via Independent Pathways That Require PBP 2." Journal of Bacteriology **191**(11): 3526.
Vijayan, S., S. Mallick, M. Dutta, M. Narayani and A. S. Ghosh (2014). "PBP Deletion Mutants of *Escherichia coli* Exhibit Irregular Distribution of MreB at the Deformed Zones." Current Microbiology **68**(2): 174-179.
Vollmer, W., D. Blanot and M. A. De Pedro (2008). "Peptidoglycan structure and architecture." FEMS Microbiology Reviews **32**(2): 149-167.
Wang, Y., B. Liu, D. Grenier and L. Yi (2019). "Regulatory Mechanisms of the LuxS/AI-2 System and Bacterial Resistance." Antimicrobial agents and chemotherapy **63**(10): e01186-01119.
Willey, J. M., K. M. Sandman and D. H. Wood (2020). Prescott's microbiology, McGraw-Hill Education.
Windels, E. M., J. E. Michiels, B. Van den Bergh, M. Fauvart and J. Michiels (2019). "Antibiotics: Combatting Tolerance To Stop Resistance." mBio **10**(5): e02095-02019.
Woldringh, C. L., Huls, P., Nanninga, N., Pas, E., Taschner, P.E.M., and Wientjes, F.B. (1988). Autoradiographic analysis of peptidoglycan synthesis in shape and cell division mutants of *Escherichia coli* LMC500. Antibiotic Inhibition of Bacterial Cell Surface Assembly and

Function. L. D. M. P. Actor, M.L. Higgins, M.R.J. Salton, and G.D. Shockman. Washington, DC, American Society for Microbiology Press**:** 66– 78.
Worthington, R. J. and C. Melander (2013). "Overcoming resistance to β-lactam antibiotics." The Journal of organic chemistry **78**(9): 4207-4213.
Young, K. D. (2006). "The Selective Value of Bacterial Shape." Microbiology and Molecular Biology Reviews **70**(3): 660-703.
Zapun, A., C. Contreras-Martel and T. Vernet (2008). "Penicillin-binding proteins and β-lactam resistance." FEMS Microbiology Reviews **32**(2): 361-385.

APPENDICES

Table 5**. Significantly regulated genes from differential sequencing of control and A22 spikes**

Common Gene Name	logFC	logCPM	PValue	FDR
ymdA b1044 JW1031	3.79732	5.313226	5.09E-29	2.02E-25
yecR b1904 JW1892	4.116968	7.582576	2.35E-26	4.67E-23
ompF cmlB coa cry tolF b0929 JW0912	4.231988	12.63258	1.48E-25	1.96E-22
kch b1250 JW1242	4.16585	2.722393	9.49E-23	9.44E-20
fliT b1926 JW1911	2.83282	5.949252	5.58E-18	4.44E-15
fliE fla AI flaN b1937 JW1921	3.130471	8.172597	1.98E-16	1.31E-13
flhB yecQ b1880 JW1869	2.886697	7.779716	2.80E-16	1.59E-13
fliS b1925 JW1910	2.695221	6.873715	4.24E-16	2.11E-13
flhE b1878 JW1867	3.160945	6.11172	5.86E-16	2.59E-13
fliO flaP flbD b1947 JW5316	2.702945	6.302795	9.75E-16	3.88E-13
fliZ yedH b1921 JW1906	2.807568	7.997627	1.15E-15	4.17E-13
fliL cheC1 fla AI fla QI b1944 JW1928	2.775557	8.962808	2.73E-15	9.05E-13
fliP flaR b1948 JW1932	2.689304	7.38503	1.24E-14	3.79E-12
fliR flaP b1950 JW1934	2.92497	5.689554	4.43E-14	1.14E-11
fliF fla AII.1 fla BI b1938 JW1922	2.768379	10.007	4.14E-14	1.14E-11
flxA b1566 JW1558	2.380647	6.89023	4.60E-14	1.14E-11

flhA b1879 JW1868	2.74421	8.761382	9.41E-14	2.20E-11
fliJ flaO flaS b1942 JW1926	2.862019	6.471341	1.51E-13	3.35E-11
cysJ b2764 JW2734	-4.44881	7.752405	1.72E-13	3.59E-11
fliH fla AII.3 fla BIII b1940 JW1924	2.717607	8.512533	2.64E-13	5.25E-11
fliI fla AIII flaC b1941 JW1925	2.678588	8.823642	5.62E-13	1.06E-10
fliQ flaQ b1949 JW1933	2.796257	4.480281	6.26E-13	1.13E-10
fliA flaD rpoF b1922 JW1907	2.632776	10.02561	8.12E-13	1.40E-10
fliK flaE flaR b1943 JW1927	3.206141	8.078321	3.58E-12	5.70E-10
cysU cysT b2424 JW2417	-3.98815	5.782937	3.58E-12	5.70E-10
fliG fla AII.2 fla BII b1939 JW1923	2.591151	9.168476	4.37E-12	6.69E-10
flgB fla FII flbA b1073 JW1060	2.654825	9.825574	4.96E-12	7.30E-10
cysD b2752 JW2722	-3.9698	6.993677	6.20E-12	8.81E-10
flgH fla FVIII flaY b1079 JW5153	2.640983	8.296826	6.46E-12	8.85E-10
spy b1743 JW1732	-1.96852	6.498999	1.60E-11	2.12E-09
fliM cheC2 fla AII fla QII b1945 JW1929	2.400703	9.256675	1.72E-11	2.14E-09
ypfG b2466 JW2450	-2.26406	4.52204	1.70E-11	2.14E-09
flgI fla FIX flaM b1080 JW1067	2.709938	8.831566	1.99E-11	2.40E-09
fliD flaV flbC b1924 JW1909	2.43978	9.161135	2.13E-11	2.50E-09
flgC fla FIII flaW b1074 JW1061	2.458395	9.026708	2.31E-11	2.62E-09
ycfJ b1110 JW1096	-2.32833	3.467865	3.33E-11	3.68E-09
flgG fla FVII flaL b1078 JW1065	2.655517	9.754651	5.19E-11	5.43E-09
ymgG b1172 JW5178	-3.15382	3.311017	5.13E-11	5.43E-09
flgJ fla FX flaZ b1081 JW1068	2.868162	8.237889	5.58E-11	5.69E-09

cysW b2423 JW2416	-3.91481	5.977122	1.09E-10	1.08E-08
amyA yedC b1927 JW1912	1.852564	6.6384	1.54E-10	1.49E-08
flgD fla FIV flaV b1075 JW1062	2.427621	10.11094	1.72E-10	1.63E-08
fliN flaN motD b1946 JW1930	2.327463	7.784766	2.25E-10	2.08E-08
ymgD b1171 JW5177	-2.50951	3.899082	2.66E-10	2.41E-08
cysN b2751 JW2721	-3.71234	7.618218	3.21E-10	2.83E-08
ftnA ftn gen-165 rsgA b1905 JW1893	1.928962	6.914107	4.16E-10	3.60E-08
bdm yddX b1481 JW5239	-4.22394	1.65261	4.59E-10	3.89E-08
cysC b2750 JW2720	-4.04594	5.59592	4.94E-10	4.09E-08
flgE fla FV flaK b1076 JW1063	2.375234	10.86102	6.59E-10	5.35E-08
ygaC b2671 JW2646	-2.05782	3.73206	7.41E-10	5.90E-08
cysP b2425 JW2418	-3.27394	7.043785	1.07E-09	8.26E-08
cysI b2763 JW2733	-4.48495	8.010176	1.08E-09	8.26E-08
ves ydjR b1742 JW1731	1.818521	5.245544	1.61E-09	1.21E-07
yaiY b0379 JW0370	-3.09808	2.169448	2.70E-09	1.99E-07
yhjG yhjF b3524 JW3492	1.715419	6.402325	3.16E-09	2.28E-07
flhC flaI b1891 JW1880	1.881425	7.060729	1.49E-08	1.06E-06
yeeE b2013 JW1995	-2.96105	6.092229	1.52E-08	1.06E-06
flgN b1070 JW1057	1.818741	6.989129	1.77E-08	1.21E-06
ivy ykfE b0220 JW0210	-1.78945	7.455756	2.17E-08	1.46E-06
flgF fla FVI flaX b1077 JW1064	2.177836	9.66771	3.63E-08	2.41E-06
ompT b0565 JW0554	1.881684	11.08758	4.57E-08	2.93E-06
cysH b2762 JW2732	-3.90777	6.836215	4.51E-08	2.93E-06

degP htrA ptd b0161 JW0157	-2.11761	10.3212	6.01E-08	3.80E-06
ydiY b1722 JW1711	1.620473	4.438103	6.84E-08	4.25E-06
ybhB b0773 JW0756	-1.48054	6.289256	1.08E-07	6.61E-06
fimI b4315 JW5779	2.071153	5.745636	1.10E-07	6.61E-06
fimC b4316 JW4279	2.437594	5.225766	1.30E-07	7.63E-06
cysA b2422 JW2415	-3.80264	7.829094	1.30E-07	7.63E-06
fliC flaF hag b1923 JW1908	1.898811	13.42878	1.36E-07	7.85E-06
fimD b4317 JW5780	2.12021	5.825681	1.96E-07	1.11E-05
flgK flaS flaW b1082 JW1069	1.754859	9.740147	2.59E-07	1.45E-05
cheW b1887 JW1876	2.407137	1.56147	2.69E-07	1.48E-05
fimA pilA b4314 JW4277	2.338373	9.658368	4.52E-07	2.46E-05
ulaG yjfR b4192 JW5868	4.009881	0.273049	5.00E-07	2.69E-05
csgD b1040 JW1023	1.981168	1.910796	5.28E-07	2.80E-05
flhD flbB b1892 JW1881	1.483852	6.314472	5.92E-07	3.10E-05
crfC yjdA b4109 JW4070	1.704856	6.880506	6.26E-07	3.22E-05
ypeC b2390 JW2387	-1.91461	3.743053	6.32E-07	3.22E-05
sufA ydiC b1684 JW1674	-1.51161	6.292903	7.84E-07	3.95E-05
yciW b1287 JW5200	-2.19558	4.419777	8.48E-07	4.22E-05
ybjI b0844 JW5113	-1.36002	6.468647	9.48E-07	4.65E-05
argB b3959 JW5553	-1.41449	5.439695	1.09E-06	5.29E-05
fimH b4320 JW4283	2.151317	4.689787	1.24E-06	5.93E-05
tsr cheD b4355 JW4318	2.363942	9.402232	1.42E-06	6.72E-05
motB b1889 JW1878	1.500289	7.89418	1.44E-06	6.73E-05
borD ybcU b0557 JW0546	2.09845	6.55485	1.57E-06	7.28E-05

flgM b1071 JW1058	1.762079	7.696388	1.67E-06	7.65E-05
pdeH yhjH b3525 JW3493	1.596654	8.285952	2.06E-06	9.30E-05
argC b3958 JW3930	-1.31452	5.926102	2.65E-06	0.000117
ygaM b2672 JW2647	-1.89611	3.137678	2.65E-06	0.000117
sufC ynhD b1682 JW1672	-1.57346	6.905722	3.11E-06	0.000136
yncE b1452 JW1447	-1.59809	9.734271	3.79E-06	0.000164
bglB b3721 JW3699	1.672618	2.227341	4.37E-06	0.000187
sufB ynhE b1683 JW5273	-1.72819	8.091408	4.46E-06	0.000189
yshB b4686 JW3839.1	1.539648	6.647638	4.98E-06	0.000208
flgL flaT flaU b1083 JW1070	1.682429	9.750148	5.05E-06	0.000209
rimL b1427 JW1423	-1.34009	4.794536	5.88E-06	0.000241
wrbA b1004 JW0989	-1.4905	5.172736	5.98E-06	0.000242
yjdM phnA b4108 JW4069	1.54748	4.437159	6.73E-06	0.00027
ynjH b1760 JW1749	1.605439	4.749635	7.84E-06	0.000312
motA flaJ b1890 JW1879	1.448566	8.483339	9.02E-06	0.000355
ygbE b2749 JW2719	-1.25014	5.669293	1.36E-05	0.000529
caiD yaaL b0036 JW0035	-1.75235	1.523325	1.82E-05	0.000702
paaZ maoC ydbN b1387 JW1382	-1.47331	3.069162	1.98E-05	0.000755
fimG b4319 JW4282	2.179843	3.46924	2.04E-05	0.000774
fimF b4318 JW4281	1.810511	2.994106	2.27E-05	0.00085
ycgR b1194 JW1183	1.386467	7.883564	2.35E-05	0.000874
ybjX b0877 JW0861	1.359763	8.470447	2.86E-05	0.001053
osmB b1283 JW1275	-1.50571	3.592095	3.26E-05	0.001191
flgA b1072 JW1059	1.662981	8.185809	3.42E-05	0.001237

paaG ydbT b1394 JW1389	-1.63645	3.318783	3.47E-05	0.001243
pdxI ydbC b1406 JW1403	-1.27071	5.302869	4.48E-05	0.001591
cspF b1558 JW1550	1.973051	1.297906	5.26E-05	0.001844
dsbG ybdP b0604 JW0597	1.376465	4.816719	5.28E-05	0.001844
osmY b4376 JW4338	-1.17786	5.900862	5.75E-05	0.00199
kdpA b0698 JW0686	1.626368	1.942382	5.87E-05	0.002014
entF b0586 JW0578	-1.50306	9.365166	6.24E-05	0.00212
sufD ynhC b1681 JW1671	-1.41324	7.902287	6.88E-05	0.0023
dsdA b2366 JW2363	-1.52503	9.36794	6.83E-05	0.0023
ybjJ b0845 JW0829	-1.09067	5.965369	7.75E-05	0.002569
pmrD b2259 JW2254	1.085269	5.660545	7.86E-05	0.002584
cadB b4132 JW4093	-1.85406	1.693405	8.91E-05	0.002905
sdaC dcrA b2796 JW2767	1.543623	10.65664	9.49E-05	0.00307
zapC ycbW b0946 JW5125	-1.41268	6.241157	9.58E-05	0.003073
acuI yhdH b3253 JW3222	-1.4709	6.503646	9.73E-05	0.003096
cheR cheX b1884 JW1873	1.156084	7.212082	0.000102	0.003215
tusA sirA yhhP b3470 JW3435	1.415637	5.780111	0.000106	0.003279
nrdI ygaO b2674 JW2649	-1.34685	5.728774	0.000106	0.003279
ybdZ b4511 JW0577	-1.36519	4.48927	0.000106	0.003279
rcsA b1951 JW1935	1.393139	4.865991	0.000109	0.003325
ynfF b1588 JW5260	-1.37133	6.608585	0.000112	0.003395
yecJ b4537 JW1891	1.562267	5.12121	0.000119	0.003572
rnpA b3704 JW3681	1.061769	6.258932	0.000129	0.003851
tcyP ydjN b1729 JW1718	-1.87265	7.530619	0.000131	0.003899

sufS csdB ynhB b1680 JW1670	-1.28451	7.52938	0.000147	0.004338
argF b0273 JW0266	-1.2172	6.301815	0.000163	0.004769
tap b1885 JW1874	1.258458	8.902773	0.00017	0.004905
yebE b1846 JW1835	-1.075	5.899064	0.00017	0.004905
yecA b1908 JW1896	-1.36442	6.713224	0.000176	0.005031
paaH ydbU b1395 JW1390	-1.57854	4.304991	0.000186	0.00529
mliC ydhA b1639 JW1631	-1.16558	3.605276	0.00019	0.005363
nrdH ygaN b2673 JW2648	-1.07188	5.566077	0.000198	0.00555
potH b0856 JW0840	-1.3636	2.467925	0.000217	0.006024
fis b3261 JW3229	1.129485	5.983349	0.00024	0.006605
sbp b3917 JW3888	-1.49549	3.681368	0.000241	0.006605
pstS phoS b3728 JW3706	1.094995	4.733207	0.000245	0.00668
yhhQ b3471 JW3436	1.273145	2.619139	0.000275	0.007436
yecD b1867 JW5307	-1.06217	7.015759	0.000282	0.00757
php yhfV b3379 JW3342	2.09094	0.499654	0.000287	0.007666
yccT b0964 JW0947	1.578279	1.586194	0.000317	0.008402
mgtA corB mgt b4242 JW4201	2.048408	6.486808	0.000338	0.008891
ubiK yqiC b3042 JW5505	1.382166	7.579431	0.000351	0.00913
aspC b0928 JW0911	-1.37065	10.23583	0.000351	0.00913
csgF b1038 JW1021	2.737266	-0.19931	0.000366	0.009463
chrR yieF b3713 JW3691	-1.03907	6.971311	0.000372	0.00955
ygiW b3024 JW2992	-1.19713	4.105232	0.000408	0.010393
yfaZ b2250 JW5371	-1.62512	5.45883	0.000455	0.011535
mcbA ybiM b0806 JW5106	1.481607	2.289846	0.000498	0.012483

nrdF ygaD b2676 JW2651	-1.11861	5.99585	0.000499	0.012483
ydiS b1699 JW1689	-1.27901	2.015002	0.000573	0.014248
yeaC b1777 JW1766	-1.20083	7.275241	0.000589	0.014547
cysM b2421 JW2414	-1.75729	6.602869	0.000595	0.014615
aldA ald b1415 JW1412	-1.38862	12.58246	0.000636	0.015516
ykfB b0250 JW0239	0.971259	6.056426	0.000645	0.015638
gabT b2662 JW2637	-1.15991	5.307213	0.000666	0.01605
lysO ybjE b0874 JW0858	1.054386	4.598413	0.000691	0.016565
kbl b3617 JW3592	-1.12563	9.630699	0.000696	0.016577
rluB yciL b1269 JW1261	0.962079	6.240064	0.000751	0.01768
ykgG b0308 JW5042	-0.94453	5.475443	0.000748	0.01768
tar cheM b1886 JW1875	1.177386	9.514468	0.000781	0.018275
sufE ynhA b1679 JW1669	-0.99272	5.421976	0.000791	0.018387
fimB b4312 JW4275	1.420231	4.760818	0.000813	0.018808
yjhQ b4307 JW4269	1.164286	2.440421	0.000852	0.019482
fes b0585 JW0576	-1.23524	7.496928	0.000851	0.019482
yjcZ b4110 JW5729	1.100168	6.831813	0.000912	0.020719
fbaB dhnA b2097 JW5344	-1.04738	5.725923	0.000951	0.021492
yjaG b3999 JW3963	1.624439	1.983288	0.000959	0.021545
moaE chlA5 b0785 JW0768	-1.33765	5.873557	0.000968	0.02163
clsC ymdC b1046 JW5150	0.910291	5.731076	0.001071	0.023785
dkgA yqhE b3012 JW5499	-1.19595	5.493736	0.001181	0.026091
yacC b0122 JW0118	1.269428	6.022652	0.001198	0.026324
cheA b1888 JW1877	1.104127	10.0205	0.001261	0.027491

nrdE b2675 JW2650	-1.14357	7.911501	0.001265	0.027491
clpA lopD b0882 JW0866	-1.35416	11.29259	0.001282	0.027716
yegS b2086 JW2070	-1.13568	2.709167	0.001343	0.028874
pfkB b1723 JW5280	-0.96345	6.795361	0.001397	0.029871
yeeO	-0.91067	4.475965	0.001421	0.030216
gadW yhiW b3515 JW3483	1.022955	5.01376	0.001434	0.030341
pdeL yahA b0315 JW0307	0.929757	3.667066	0.001449	0.030465
katG b3942 JW3914	-1.09262	10.7292	0.001463	0.030465
cbl b1987 JW1966	-1.18799	3.621683	0.001463	0.030465
fcl wcaG yefB b2052 JW2037	-1.70333	0.834743	0.001479	0.030635
entA b0596 JW0588	-1.36177	6.086403	0.001493	0.030767
yehI b2118 JW2105	1.163157	2.811656	0.00158	0.032385
dicA b1570 JW1562	1.405175	6.472655	0.001592	0.03246
aer air yqjJ b3072 JW3043	1.094665	8.577912	0.001609	0.032648
yjcS b4083 JW5721	1.424115	1.281893	0.00169	0.033936
nlpD b2742 JW2712	-1.58491	9.894384	0.001685	0.033936
glxK glxB5 ybbZ b0514 JW0502	-1.4544	2.763363	0.001705	0.034075
yjfN b4188 JW5742	-1.07069	2.745813	0.001766	0.035126
patD prr ydcW b1444 JW1439	-0.92501	4.072417	0.001778	0.035171
sdaB b2797 JW2768	1.27786	9.758298	0.001862	0.036535
sad yneI b1525 JW5247	-0.90401	5.879531	0.00187	0.036535
gsiA yliA b0829 JW5897	-1.14787	8.046921	0.001874	0.036535
yicH b3655 JW3630	1.397111	1.379755	0.001887	0.0366
lsrD ydeZ b1515 JW1508	-1.28538	2.836389	0.001944	0.037536

cmtB b2934 JW2901	1.780707	0.53215	0.001965	0.03776
yjdP b4487 JW5890	-0.96185	3.753725	0.002119	0.040323
ytfK b4217 JW5749	-1.055	6.842558	0.002117	0.040323
sstT ygjU b3089 JW3060	0.958249	7.082633	0.002187	0.040917
ybbP b0496 JW0485	-0.95939	5.887573	0.002191	0.040917
cysK cysZ b2414 JW2407	-1.3916	11.06798	0.00218	0.040917
nanK yhcI b3222 JW5538	-1.61061	8.183581	0.002176	0.040917
gsiB yliB b0830 JW5111	-1.28405	7.458824	0.002229	0.041415
yagP	1.278733	1.24594	0.002319	0.04242
ycaM b0899 JW5119	1.004574	3.68666	0.002336	0.04242
nemA ydhN b1650 JW1642	-0.84641	6.455065	0.002319	0.04242
yceM mviM b1068 JW1055	-0.92955	6.896791	0.002331	0.04242
hisH b2023 JW2005	-1.41546	5.444641	0.002335	0.04242
ybbA b0495 JW0484	-1.49313	4.985885	0.002373	0.04289
dsdX orf445 yfdA yfdD b2365 JW2362	-2.43688	7.167037	0.002408	0.043327
yeaG b1783 JW1772	-0.89341	4.5506	0.002446	0.043613
hslJ ydbI b1379 JW1374	-1.01939	5.049103	0.002437	0.043613
lsrR ydeW b1512 JW1505	-1.0655	4.692295	0.002502	0.044418
lpxT yeiU b2174 JW2162	0.852507	5.502663	0.00253	0.044718
yodB b1974 JW5323	1.468601	1.31654	0.002573	0.045279
kduD ygeC yqeD b2842 JW2810	-0.83354	4.705996	0.002659	0.046582
ybgQ b0718 JW5099	1.208401	2.848866	0.002694	0.046995
btuC b1711 JW1701	-0.82621	5.871067	0.002719	0.047223

plaP yeeF b2014 JW5330	0.953673	5.346125	0.002833	0.048833
cobS b1992 JW1970	-1.3055	5.245175	0.002836	0.048833

Table 5**. Significantly regulated genes from differential sequencing of control and A22 spikes:** A22 (10 μg/ml) was added at an $O.D._{600}$~0.1 and grown for one hour post spike before RNA extractraction. Control cells were grown for four hours before RNA extraction. Log fold change in A22* condition shown relative to control. Only genes significantly regulated by FDR shown.

Table 6. **Significantly regulated genes from differential sequencing of control and mecillinam spikes**

Common Gene Name	logFC	logCPM	PValue	FDR
ompF cmlB coa cry tolF b0929 JW0912	3.441708	12.6769	7.68E-15	3.05E-11
ymgG b1172 JW5178	-3.52771	3.62346	5.93E-13	1.18E-09
ycfJ b1110 JW1096	-2.61158	3.686899	3.76E-11	4.98E-08
flxA b1566 JW1558	2.276043	6.901069	1.85E-10	1.84E-07
cysI b2763 JW2733	-3.47585	7.055778	3.12E-10	2.41E-07
degP htrA ptd b0161 JW0157	-2.70128	10.793	3.64E-10	2.41E-07
cysH b2762 JW2732	-2.80432	5.831676	1.20E-08	6.81E-06
ymgD b1171 JW5177	-2.75208	4.086832	1.95E-08	9.69E-06
bdm yddX b1481 JW5239	-3.80913	1.266779	2.06E-07	9.11E-05
cysC b2750 JW2720	-2.85407	4.506044	4.81E-07	0.000174
cysJ b2764 JW2734	-3.5456	6.898248	4.86E-07	0.000174
fimI b4315 JW5779	2.244485	5.715277	5.86E-07	0.000174
cysN b2751 JW2721	-2.67084	6.676498	5.93E-07	0.000174
fimC b4316 JW4279	2.555392	5.213756	6.13E-07	0.000174
flhC flaI b1891 JW1880	1.740896	7.086439	6.79E-07	0.00018
ompG b1319 JW1312	3.892114	0.329686	2.80E-06	0.000695
spy b1743 JW1732	-1.81274	6.368563	3.80E-06	0.000889
fliT b1926 JW1911	1.575651	6.17072	7.26E-06	0.001603
fimD b4317 JW5780	2.00666	5.849152	9.42E-06	0.001971
cysD b2752 JW2722	-2.97771	6.086246	1.14E-05	0.002189
ypfG b2466 JW2450	-1.72715	4.088547	1.16E-05	0.002189

fimA pilA b4314 JW4277	2.132043	9.695858	1.35E-05	0.002434
cysW b2423 JW2416	-3.20504	5.323471	1.42E-05	0.00245
flhD flbB b1892 JW1881	1.420791	6.321353	1.71E-05	0.002837
ves ydjR, b1742, JW1731	1.505191	5.312364	1.79E-05	0.002844
yaiY b0379 JW0370	-2.61854	1.776562	1.88E-05	0.002866
osmB b1283 JW1275	-1.85176	3.845885	1.96E-05	0.002881
fimH b4320 JW4283	2.185876	4.689777	2.06E-05	0.002926
caiD yaaL b0036 JW0035	-2.07089	1.724169	2.14E-05	0.002929
fliC flaF hag b1923 JW1908	1.65778	13.47586	2.78E-05	0.003677
yebE b1846 JW1835	-1.38969	6.105887	3.13E-05	0.003915
ycgR b1194 JW1183	1.544239	7.835907	3.15E-05	0.003915
cysU cysT b2424 JW2417	-3.12272	4.987973	3.45E-05	0.004151
cysA b2422 JW2415	-2.77398	6.897588	3.68E-05	0.0043
amyA yedC b1927 JW1912	1.391263	6.744334	5.00E-05	0.005674
ygaC b2671 JW2646	-1.49894	3.293888	5.84E-05	0.006449
ynjH b1760 JW1749	1.652494	4.73904	9.40E-05	0.010016
yecR b1904 JW1892	1.541113	7.923851	9.58E-05	0.010016
ypeC b2390 JW2387	-1.65413	3.535262	0.000102	0.010364
cheR cheX b1884 JW1873	1.338806	7.145017	0.000134	0.013317
fruB fpr fruF b2169 JW2156	-1.57327	5.353058	0.000146	0.014009
fliD flaV flbC b1924 JW1909	1.504926	9.341945	0.000148	0.014009
fliS b1925 JW1910	1.353389	7.136356	0.000155	0.014111
ulaG yjfR b4192 JW5868	2.69309	0.412034	0.000156	0.014111
ivy ykfE b0220 JW0210	-1.2454	7.043501	0.000162	0.014296

motB b1889 JW1878	1.35596	7.923381	0.000172	0.014829
yhjG yhjF b3524 JW3492	1.28131	6.504702	0.000175	0.014829
motA flaJ b1890 JW1879	1.381733	8.492104	0.00024	0.019879
yacC b0122 JW0118	1.590567	5.937734	0.00025	0.020301
fcl wcaG yefB b2052 JW2037	-2.66602	1.512654	0.000255	0.020301
fimG b4319 JW4282	2.06645	3.502478	0.000276	0.021529
crfC yjdA b4109 JW4070	1.329289	6.97138	0.000386	0.02952
ygaM b2672 JW2647	-1.64071	2.921861	0.000415	0.031126
ybhB b0773 JW0756	-1.19136	6.070594	0.000427	0.031126
yehI b2118 JW2105	1.452694	2.735235	0.000431	0.031126
yhbO b3153 JW5529	-1.90195	0.936514	0.00044	0.031209
pgaB ycdR b1023 JW5142	1.631562	1.894816	0.000455	0.031718
ygiM b3055 JW3027	-1.25006	7.494119	0.000465	0.031865
ompN ynaG b1377 JW1371	1.418481	11.63031	0.000503	0.033873
fabB fabC b2323 JW2320	-1.3409	11.44471	0.000521	0.034067
fimF b4318 JW4281	1.778017	3.012359	0.000523	0.034067
ubiK yqiC b3042 JW5505	1.467135	7.556633	0.000612	0.039235
ybgQ b0718 JW5099	1.644903	2.73852	0.000651	0.041046

Table 6**. Significantly regulated genes from differential sequencing of control and mecillinam spikes:** Mecillinam(3 μg/ml) was added at an $O.D._{600}$~0.1 and grown for one hour post spike before RNA extraction. Control cells were grown for four hours before RNA extraction. Log fold change in mec* condition shown relative to control. Only genes significantly regulated by FDR shown.

VITA

Addison Grinnell

Candidate for the Degree of

Master of Science

Thesis: A DENSITY-DEPENDENT MECHANISM FOR ANTIBIOTIC TOLERANCE IN ROD BACTERIA

Major Field: Microbiology, Cell and Molecular Biology

Biographical:

Education:

Completed the requirements for the Master of Science in Microbiology, Cell and Molecular Biology at Oklahoma State University, Stillwater, Oklahoma in July, 2021

Completed the requirements for the Bachelor of Science in Biological Science at Oklahoma State University, Stillwater, Oklahoma in 2018.

Presentations at Academic and Professional Meetings:

Addison Grinnell, Ryan Sloan, and Randy Morgenstein. A density-dependent requirement of PBP1B for cells to grow after disruption of the MreB-PBP2 elongation complex requires a minimum cell density. Annual ASM Missouri and Missouri Valley Branch meeting, Virtual. March 20, 2021.